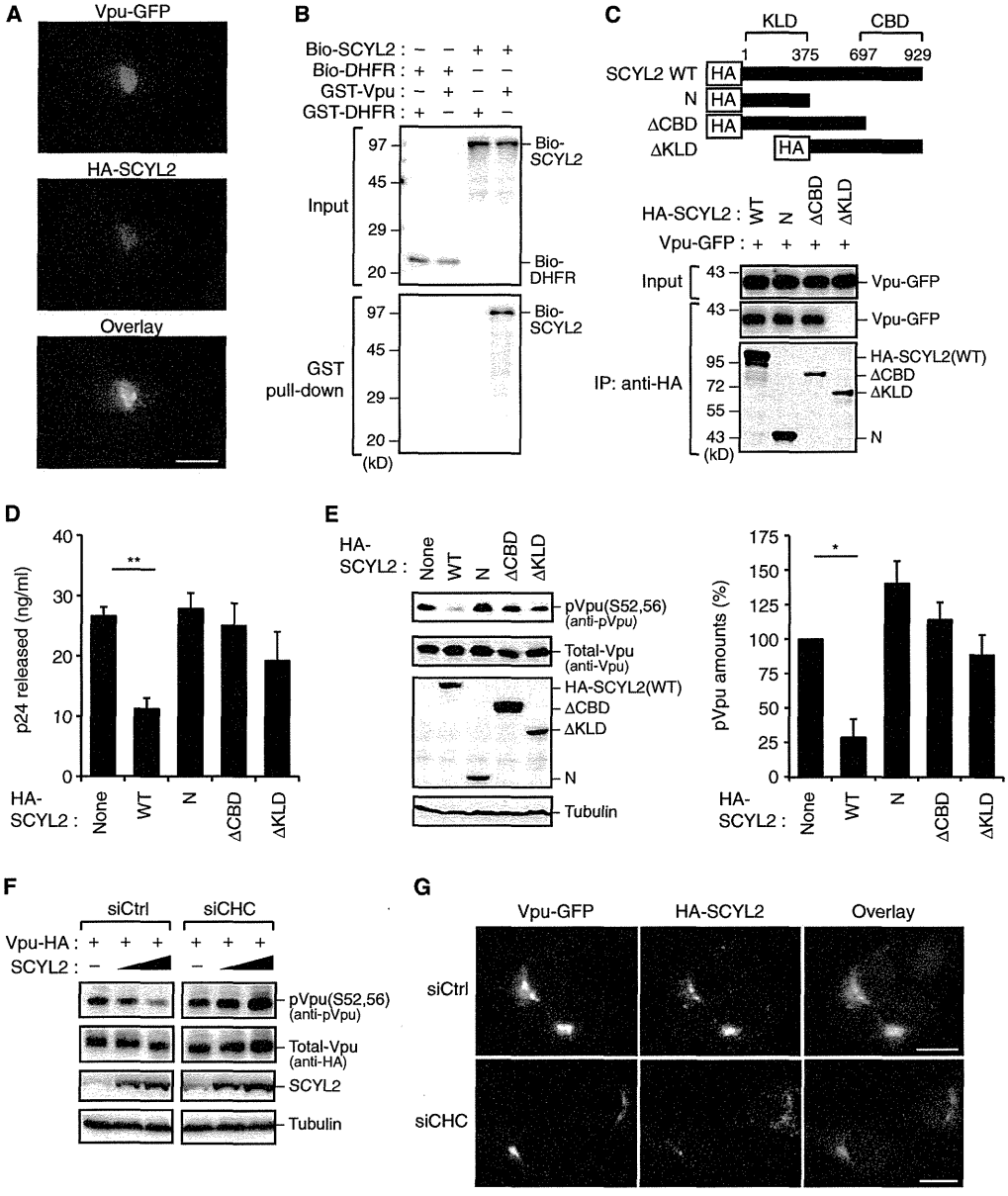


**Fig. 5.** Both the KLD and CBD of SCYL2 are required for its ability to antagonize Vpu activity. (**A**) Colocalization of Vpu and SCYL2 in cells. HeLa cells were transfected with plasmids encoding Vpu-GFP and HA-SCYL2. After 24 hours, the cells were fixed, permeabilized, and stained with anti-HA antibody (red), followed by confocal microscopic analysis. Nuclei were stained with 4′,6-diamidino-2-phenylindole (DAPI) and are shown in blue. Scale bar, 10 μm. (**B**) SCYL2 interacts with Vpu in vitro. Recombinant biotinylated SCYL2 (Bio-SCYL2) and biotinylated dihydrofolate reductase (Bio-DHFR) were processed for GST pull-down analysis with either GST-Vpu or GST-DHFR. DHFR was used as a negative control. Captured proteins were analyzed by Western blotting with streptavidin-HRP. (**C**) The N-terminal KLD of SCYL2 interacts with Vpu. HEK 293T cells were cotransfected with plasmids encoding Vpu-GFP together with plasmid encoding WT SCYL2 or one of its truncation mutants. Cell lysates were immunoprecipitated (IP) with anti-HA antibody and then analyzed by Western blotting with anti-GFP or anti-HA antibodies. (**D** and **E**) SCYL2 mutants lacking the CBD have no observable effect on (D) viral release or (E) Vpu dephosphorylation. Cells were cotransfected with pNL4-3 (100 ng) together with the indicated SCYL2 expression plasmids (100 ng). Forty-eight hours after transfection, culture supernatants and cell lysates were subjected to (D) p24 ELISA or (E) Western blotting analysis with anti-pVpu, anti-Vpu, anti-HA, and anti-tubulin antibodies. The bar chart in (E) indicates the amounts of pVpu as determined by densitometric analysis of Western blots. $^{**}P$ = 0.0045; $^{*}P$ = 0.0172; $n$ = 3 experiments. (**F**) CHC depletion abrogates SCYL2-mediated dephosphorylation of Vpu. HEK 293T cells were treated with either control (siCtrl) or CHC-targeted siRNA (siCHC) for 24 hours before being transfected with plasmids expressing Vpu-HA and SCYL2 at a molar ratio of 1:5 or 1:10. Forty-eight hours after transfection, cell lysates were subjected to Western blotting with the indicated antibodies. (**G**) CHC depletion interferes with the colocalization of SCYL2 and Vpu. HeLa cells were treated with either control or CHC-specific siRNA for 24 hours before being transfected with plasmids encoding Vpu-GFP and HA-SCYL2. After 24 hours, the cells were fixed, permeabilized, stained with anti-HA antibody (red), and analyzed by confocal microscopy. Nuclei were stained with DAPI (blue). Scale bars, 10 μm. Data shown in (A) to (C) and (E) to (G) are representative of three experiments.

SCYL2 was transactivated by IFN-β (Fig. 7B). We next examined whether type I IFN promoted the SCYL2-mediated dephosphorylation of Vpu. To this end, we infected HeLa and H9 cells with vesicular stomatitis virus glycoprotein (VSVG)–pseudotyped HIV-1 and then treated the cells with IFN-β. As expected, the addition of IFN-β induced the dephosphorylation of Vpu (Fig. 7C). Single-cycle virus release analysis revealed that IFN-β decreased the amounts of virus released (Fig. 7D), as reported previously (*41*). However, the targeted depletion of SCYL2 by siRNA partially blocked IFN-β–mediated viral restriction (Fig. 7D). This was not the case in parallel experiments with Vpu-deficient viruses or BST2-deficient cells (Fig. 7, E and F). Together,

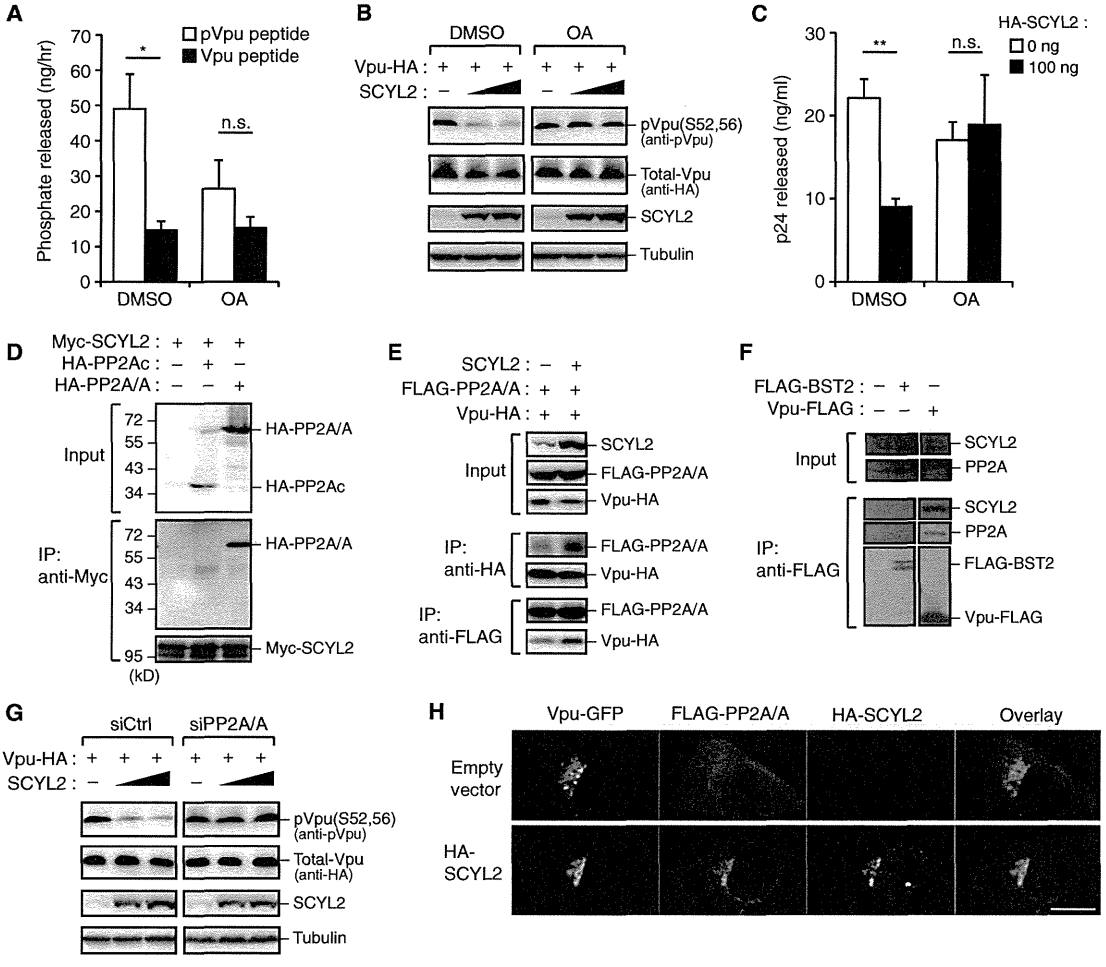


Fig. 6. SCYL2 promotes PP2A-mediated dephosphorylation of Vpu. (A) SCYL2 immunoprecipitates have phosphatase activity toward $Ser^{52}$ and $Ser^{56}$ on Vpu. HEK 293T cells expressing HA-SCYL2 were lysed and subjected to immunoprecipitation with an anti-HA antibody in buffer containing dimethyl sulfoxide (DMSO) or 10 nM OA. The immunoprecipitates were incubated with either pVpu peptide (white bar) or the nonphosphorylated equivalent (black bar). After 8 hours, the amounts of released phosphates in the reaction mixture were measured. n.s., not significant; $^*P = 0.0410$; $n = 3$ experiments. (B) OA inhibits the SCYL2-mediated dephosphorylation of Vpu. HEK 293T cells were transfected with plasmids expressing Vpu-HA and SCYL2 at a molar ratio of 1:5 or 1:10. Cells were treated with DMSO or 10 nM OA for 18 hours before being harvested. Forty-eight hours after transfection, cell lysates were subjected to Western blotting with the indicated antibodies. (C) OA blocks SCYL2-mediated restriction of viral release. HeLa cells were cotransfected with pNL4-3 (100 ng) with or without plasmid encoding SCYL2. Cells were then treated with DMSO control or 10 nM OA for 18 hours before being harvested. Forty-eight hours after transfection, culture supernatants were subjected to p24 ELISA. n.s., not significant; $^{**}P = 0.0039$; $n = 3$ experiments. (D) SCYL2 interacts with the scaffold A subunit of PP2A (PP2A/A). HEK 293T cells were transfected with expression plasmids for the indicated proteins. Cell lysates were immunoprecipitated with an anti-Myc antibody, and bound proteins were visualized by Western blotting. (E) SCYL2 enhances the interaction between Vpu and PP2A/A. HEK 293T cells were transfected with vectors encoding the indicated proteins. Cell lysates were immunoprecipitated with anti-HA or anti-FLAG antibodies, and bound proteins were visualized by Western blotting analysis. (F) Vpu interacts with endogenous SCYL2 and PP2A. HEK 293T cells were transfected with vectors encoding the indicated proteins. Cell lysates were immunoprecipitated with anti-FLAG antibody, and bound proteins were visualized by Western blotting analysis. (G) Depletion of PP2A/A inhibits SCYL2-mediated dephosphorylation of Vpu. HEK 293T cells were treated with either control (siCtrl) or PP2A/A-specific siRNA (siPP2A/A) for 24 hours before being transfected with plasmids expressing Vpu-HA and SCYL2 at molar ratios of 1:5 and 1:10. Forty-eight hours after transfection, cell lysates were subjected to Western blotting with antibodies against the indicated proteins. (H) Immunofluorescence analysis of HeLa cells transiently coexpressing Vpu-GFP (green), FLAG-PP2A/A (red), and either HA-SCYL2 (blue) or empty vector. Scale bar, 10 μm. Data shown in (B) and (D) to (H) are representative of three experiments.

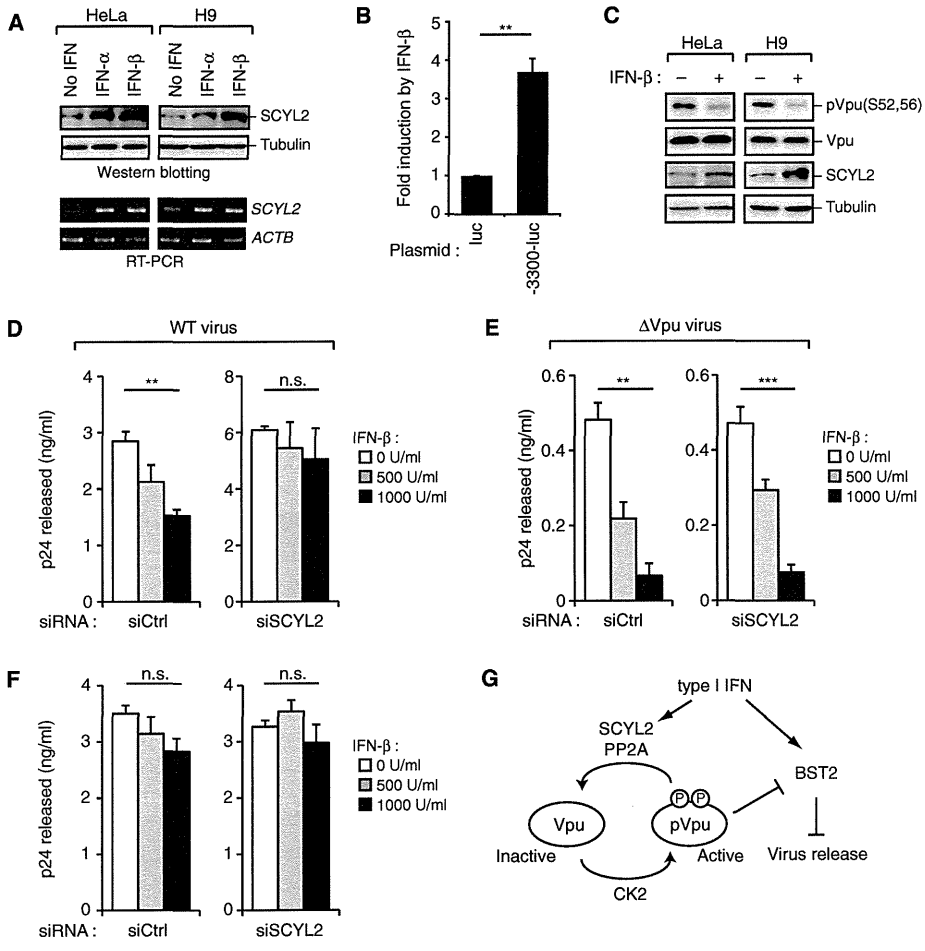


Fig. 7. SCYL2 mediates the type I IFN–induced antiviral response. (A) Type I IFN increases the abundance of SCYL2. Western blotting analysis (top) and RT-PCR analysis (bottom) of the indicated cells treated with IFN-α or IFN-β (1000 U/ml) for 6 hours before harvesting. Representative data from three experiments are shown. (B) The SCYL2 promoter is transactivated by IFN-β. HeLa cells were cotransfected with the pGL4-luc vector encoding SCYL2 promoter (-3300-luc) together with pGL4-TK-Rluc as a transfection control. Forty-eight hours after transfection, cells were treated with IFN-β (1000 U/ml) for 6 hours and cell lysates were subjected to a luciferase reporter assay. The fold induction in IFN-treated cells was determined. $^{**}P = 0.0036$; $n = 3$ experiments. (C) IFN-β induces Vpu dephosphorylation in infected T cells. The indicated cells were infected with VSVG-pseudotyped HIV-$1_{NL4-3}$ [at a multiplicity of infection (MOI) of 0.2] and treated with IFN-β (1000 U/ml) for 8 hours before being harvested. Cell lysates were subjected to Western blotting with antibodies against the indicated proteins. Data are representative of three experiments. (D to F) SCYL2 depletion partially blocks the antiviral effect of IFN-β. (D and E) HeLa cells or (F) BST2-knockdown HeLa cells were treated with either control or SCYL2-specific siRNA for 24 hours before being infected with (D and F) VSVG-pseudotyped HIV-$1_{NL4-3}$ or (E) its Vpu-deficient derivative at an MOI of 0.01. Forty-eight hours after infection, the cells were washed and treated with IFN-β (0, 500, or 1000 U/ml) for 8 hours. Culture supernatants and cell lysates were subjected to p24 ELISA. n.s., not significant; $^{**}P = 0.0079$ for (D); $^{**}P = 0.0012$ and $^{***}P = 0.0007$ for (E); $n = 3$ experiments. (G) A model depicting the proposed signaling cascade in type I IFN–mediated viral release restriction. Type I IFN induces the production of both BST2 and SCYL2 in infected cells. SCYL2 binds to Vpu, recruits PP2A, and inhibits the anti-BST2 activity of Vpu, thereby facilitating the BST2-mediated restriction of viral release.

these observations indicated that SCYL2 is itself IFN-inducible, and that by antagonizing Vpu function and consequently facilitating BST2-mediated restriction, SCYL2 stimulates the anti-HIV activity of type I IFN (Fig. 7G).

## DISCUSSION

Here, we demonstrated that SCYL2 is an IFN-inducible gene that regulates the phosphorylation of HIV-1 Vpu by recruiting PP2A to the viral protein, thereby inhibiting Vpu function and enhancing the antiviral activity of BST2 in HIV-1–infected cells. SCYL2 was originally identified as a poly-L-lysine–stimulated kinase that phosphorylates the β2 subunit of the adaptor protein AP-2 (*50*). Although the idea of whether SCYL2 has kinase activity is still controversial (*52*), a subsequent study suggested that SCYL2 is a multifunctional protein involved in membrane trafficking between the *trans*-Golgi and endosomes (*51*). Other studies have reported a role for SCYL2 in the clathrin-mediated sorting of t-SNARE (target-soluble *N*-ethylmaleimide–sensitive factor attachment protein receptor) proteins (*52*) and in the Wnt signaling pathway (*59*). Here, we reveal an additional role for SCYL2 as an inhibitor of viral release in HIV-1–infected cells through its inhibition of the phosphorylation of Vpu.

A study predicted the existence of at least 4000 as yet unidentified phosphorylation sites on hundreds of viral proteins (*60*). Indeed, the phosphorylation of viral proteins is one of the most important processes for efficient viral replication and pathogenesis (*61*). Previous biochemical analyses have reported that the phosphorylation of Vpu on key serine residues ($Ser^{52}$ and $Ser^{56}$) is catalyzed by CKII (*29–31*). Because CKII is a ubiquitously expressed serine and threonine (Ser/Thr) kinase (*62*), the $Ser^{52}$ and $Ser^{56}$ phospho-acceptor sites are likely to be constitutively phosphorylated in infected cells, suggesting that dephosphorylation could be a key step for exerting control over Vpu function. However, the sequence requirements of major cellular phosphatases are less specific than those of protein kinases (*63*), and additional cofactors are likely needed for phosphatases to target a specific substrate. Indeed, many transporter or adaptor proteins interact with subunits of phosphatases to promote substrate recognition by these dephosphorylating enzymes (*64*).

Although the phosphorylation of Vpu is required for optimal anti-BST2 activity, the precise molecular mechanism by which the phosphorylation status of Vpu is controlled has been elusive. The association of SCYL2 with both Vpu and PP2A suggests a previously unrecognized mechanism through which the activity of Vpu is regulated by SCYL2-mediated recruitment of PP2A and dephosphorylation. Our data suggest that SCYL2 induces the dephosphorylation

of Vpu, abrogating Vpu function and consequently inhibiting viral particle release through BST2. Our model of the SCYL2-PP2A-Vpu virus-host interaction is reminiscent of previously described interactions among cellular proteins; for example, cyclin G recruits PP2A to Mdm2 in a similar manner to facilitate the dephosphorylation and functional modification of Mdm2 (*65*).

Our model, however, does not directly address the original role of SCYL2 as a component of clathrin-coated vesicles. Although the role of clathrin during Vpu-induced BST2 inactivation is still uncertain, substantial data suggest that a clathrin-dependent pathway contributes to the antagonism of BST2 by Vpu (*19*, *24*, *66*, *67*). On the basis of our present findings that clathrin is required for SCYL2 function with respect to Vpu, SCYL2 could conceivably inhibit Vpu by modulating clathrin-mediated membrane trafficking. Of note in this regard, several studies have proposed that Vpu counteracts BST2 at least partly through a β-TrCP–independent (phosphorylation-independent) pathway (*54*, *55*). Indeed, we observed that SCYL2 interacted with a nonphosphorylated mutant of Vpu, as well as with wild-type Vpu, implying that SCYL2 might interfere with the anti-BST2 activity of Vpu irrespective of the phosphorylation status of Vpu. However, the phosphatase inhibitor OA almost completely abrogated the activity of SCYL2. Moreover, SCYL2 did not affect the virion release of an HIV-1 derivative encoding a nonphosphorylatable form of Vpu. Together, these results suggest that the function of SCYL2 as a Vpu inhibitor is likely dependent on the phosphorylation of the Vpu residues $Ser^{52}$ and $Ser^{56}$.

Our data indicate that human SCYL2 has no obvious efficacy against ancestral Vpu, which suggests that the SCYL2-Vpu interaction might have appeared during the evolution of primate lentiviruses. However, whether SCYL2 from GSN monkeys might interfere with $SIV_{GSN}$ Vpu and whether primate SCYL2 has evolved to gain an antagonistic interaction with HIV-1 Vpu are currently unresolved questions. How can the acquisition of SCYL2-binding activity by HIV-1 Vpu be reconciled with the seemingly inhibitory function of SCYL2 on HIV-1 release? One possibility is that the SCYL2-Vpu interaction is associated with an unrecognized benefit in some aspect of the viral life cycle. For example, SCYL2 might increase the stability of Vpu through dephosphorylation. Indeed, a previous report suggested that nonphosphorylated Vpu is more stable than wild-type Vpu (*68*). Another possibility is that the cycle of phosphorylation and dephosphorylation is important for Vpu activity. Nonetheless, our observation that overexpression of SCYL2 inhibits the antagonism of BST2 by Vpu, whereas depletion of endogenous SCYL2 has the opposite effect, suggests that, at least with regard to this function, SCYL2 behaves as an inhibitor rather than a cofactor of Vpu.

In addition to BST2, several factors induced by type I IFN contribute to viral restriction during the late stages of virus assembly and release. For example, the ubiquitin-like protein ISG15 specifically inhibits the ubiquitination of Gag and its association with Tsg101, resulting in the restriction of HIV-1 budding (*40*). A tripartite motif (TRIM) protein, TRIM22, is another ISG that blocks HIV-1 assembly by disrupting the proper trafficking of Gag to the plasma membrane (*41*). These restrictions are Vpu-independent mechanisms because these factors either interact with Gag or modulate its function. Our data demonstrate that type I IFN can also trigger the dephosphorylation of Vpu through SCYL2 and thereby facilitate BST2-mediated viral restriction even in the presence of Vpu, implying a regulatory role for SCYL2 among the array of IFN-mediated antiviral host measures. In conclusion, our current study provides evidence that the IFN-mediated antiviral response targets the posttranslational modification of Vpu and contributes to the inhibition of HIV-1 release from infected cells. The molecular machinery underlying the posttranslational modification of Vpu may thus be an attractive therapeutic target for the treatment of HIV infection.

## MATERIALS AND METHODS

### In vitro protein production

A total of 412 complementary DNAs (cDNAs) encoding human protein kinases were constructed as described previously (*69*). The protein production method has been described previously (*42*, *70*, *71*). Briefly, DNA templates containing a biotin-ligating sequence were amplified by split-PCR with cDNAs and corresponding primers and then used with the GenDecoder protein production system (CellFree Science). For synthesis of HIV-1 Vpu protein, *vpu* genes derived from the pNL4-3 proviral plasmid (*72*) were generated by split-PCR and used as templates with the Wheat Germ Expression Kit (CellFree Science) in accordance with the manufacturer's instructions.

### AlphaScreen-based protein-protein interaction assays

FLAG-tagged Vpu proteins were mixed with biotinylated kinases in 15 μl of reaction buffer [20 mM tris (pH 7.6), 5 mM $MgCl_2$, 1 mM dithiothreitol] in a well of 384-well optiplates (PerkinElmer) and incubated at 26°C for 1 hour. The mixture was then added to AlphaScreen buffer containing anti–immunoglobulin G (protein A) acceptor beads and streptavidin-coated donor beads (0.1 μl each; PerkinElmer) and the anti-FLAG M2 antibody (5 μg/ml; Sigma) and further incubated at 26°C. One hour later, AlphaScreen signals from the mixture were detected with an EnVision device (PerkinElmer) with the AlphaScreen signal detection program.

### Cells and transfections

HEK 293T, HeLa, LLC-MK2, Jurkat, and H9 cells were cultured under standard conditions. Plasmid or siRNA transfection into adherent cells was performed with the Effectene or Hiperfectamine transfection reagent (Qiagen), respectively, in accordance with the manufacturer's instructions. Transfection of suspension cells with plasmids was performed with the Neon Transfection System (Invitrogen) according to the manufacturer's protocol.

### Plasmids and viruses

Human SCYL2 (GenBank accession no. BC063798) full-length sequences (1 to 929 amino acid residues) and deletion inserts (1 to 375, 1 to 697, and 376 to 929 amino acids) were amplified from pCMV6-XL4-SCYL2 (Origene) with primer pairs containing restriction enzyme sites and a stop codon. These inserts were subcloned into pCMV-HA/pCMV-Myc vector (Clontech). Alternatively, on the basis of bioinformatic predictions, the 3.3-kb fragment upstream of the SCYL2-encoding gene was amplified from HEK 293T cDNA and subcloned into the pGL4.10 firefly luciferase reporter vector (Promega). A human codon-optimized HIV-1 Vpu expression vector (*73*) and a Vpu-deleted HIV-1 molecular clone (*74*) were provided by K. Strebel [National Institutes of Health (NIH), Bethesda, MD]. The Vpu(S52,56A) mutants were constructed with standard molecular cloning procedures. The construct encoding KSHV-K5 (*75*) was provided by P. Cannon (University of Southern California, Los Angeles, CA). The plasmids expressing PP2A/A and $PP2A_C$ (*76*) were provided by A. Yamashita (Yokohama City University, Kanagawa, Japan). The VSVG-pseudotyped virus stocks were produced by transient transfection of HEK 293T cells with the pNL4-3 proviral clone and vectors expressing VSVG at a molar ratio of 3:1. After 48 hours, the culture supernatants containing virus were collected, filtered through a 0.45-μm Millex-HV filter (Millipore), and immediately stored at −80°C until required.

### siRNA, IFN treatments, and RT-PCR

An array of siRNAs targeting the genes shown in Fig. 1D, as well as BST2, CHC, and PP2A/A, was obtained from Qiagen and used as a mixture of three different targeting sequences. In experiments involving SCYL2 knockdown, we used at least two SCYL2-specific Stealth RNAi constructs (oligo ID

HSS124796 and HSS183194, Invitrogen) to avoid off-target effects. Stealth RNAi Luciferase Reporter Control (Invitrogen) was used as the negative control. For detection of SCYL2 mRNA in IFN-treated cells, total RNA was extracted with the RNeasy Mini Kit (Qiagen) from cells treated with or without recombinant human IFN-α (1000 U/ml; Sigma) or IFN-β (1000 U/ml; PBL Biomedical Laboratories) for 6 hours before harvesting. The cDNA was generated with ReverTra Ace (Toyobo) and an oligo$(dT)_{20}$ primer, and then PCR was performed with Ex Taq (Takara Bio). The PCR primers used were as follows: *SCYL2*, 5′-gggaatcagcaaattgacaaagttt-3′ (forward) and 5′-agtccttagtctgtttaacagtagc-3′ (reverse); *ACTB*, 5′-ggacttcgagcaagagatgg-3′ (forward) and 5′-agcactgtgttggcgtacag-3′ (reverse).

### Single-cycle virus release assays

For transfection-based assays, cells in 12-well plates were cotransfected with pNL4-3 or pNL4-3ΔVpu (100 ng) and either an SCYL2 expression vector or an empty vector (0, 50, and 100 ng) and cultured for 2 days. For infection-based assays, cells were infected with the VSVG-pseudotyped HIV-1 at an MOI of 0.01 or 0.2 for 8 hours and cultured for 2 days (HeLa cells) or 4 days (H9 cells). In experiments with siRNA, cells were transfected with a pool of siRNAs 24 hours before being either transfected with pNL4-3 or infected with virus. Virus-containing supernatants were harvested and filtered to remove debris, and viral p24 antigens were measured with an ELISA kit (Zepto Metrix). The cell lysates were prepared with HBST buffer [10 mM Hepes (pH 7.4), 150 mM NaCl, 0.5% Triton X-100] containing protease inhibitor cocktail (Roche). Western blotting analysis and the antibodies used have been described previously (*77*). In some experiments, OA (Calbiochem) was added 18 hours before harvesting. In experiments with IFN-β, virus-producing cells were washed twice with phosphate-buffered saline (PBS) and treated with IFN-β for 8 hours before being harvested. The culture supernatants and cell lysates were subjected to p24 ELISA measurement or Western blotting analysis, as described earlier.

### Flow cytometry

Cells in 12-well plates were transfected with vectors encoding Vpu (100 ng), green fluorescent protein (GFP) (100 ng), and either HA-SCYL2 or empty plasmid (0, 1, and 2 μg). Alternatively, vector encoding KSHV-K5 was used instead of vector encoding Vpu. Eighteen hours later, cells were harvested in PBS containing 5 mM EDTA and washed with PBS containing 1% bovine serum albumin (BSA). The cells were blocked with 10% normal goat serum and then stained with an anti-BST2 antibody (a gift from Chugai Pharmaceutical Co.) and a phycoerythrin (PE)–conjugated secondary antibody (Beckman Coulter) or a PE/Cy7-conjugated anti-CD4 antibody (BioLegend). All samples were fixed with 4% paraformaldehyde and analyzed with a FACSCanto II instrument (BD Biosciences) and FlowJo software (Treestar) gated for the GFP-positive fraction.

### Detection of pVpu

For phosphate-affinity (Phos-tag) gel analysis, cells in 12-well plates were transfected with vectors encoding either wild-type Vpu or the Vpu(S52,56A) mutant (100 ng) together with plasmid encoding SCYL2 (at 0, 500, or 1000 ng). Two days later, cell lysates were loaded onto an 8% polyacrylamide gel containing 50 μM $MnCl_2$ and 25 μM Phos-tag acrylamide (Wako). After electrophoresis, gels were soaked in a general transfer buffer with 1 mM EDTA for 10 min to eliminate $Mn^{2+}$ ions and then subjected to Western blotting analysis with anti-Vpu antibody (a gift from K. Strebel). A phospho-specific polyclonal antibody against Vpu phosphorylated at $Ser^{52}$ and $Ser^{56}$ was produced and purified by Scrum Inc.

### Microscopy

One day before transfection, cells were seeded onto glass-bottomed dishes (Matsunami). At 48 hours after transfection, the cells were fixed and stained as described previously (*77*). Microscopic imaging was performed with an FV1000-D confocal laser scanning microscope (Olympus) equipped with a 60× oil-immersion objective.

### In vitro and in vivo binding assays

For in vitro GST pull-down assays, biotinylated SCYL2 was incubated with either GST-Vpu or GST–dihydrofolate reductase (DHFR) at 26°C for 2 hours before being co-incubated with glutathione-Sepharose beads (GE Healthcare) at 4°C for 3 hours. The beads were then washed three times, and bound proteins were analyzed by Western blotting with streptavidin–horseradish peroxidase (HRP) conjugate (GE Healthcare). For immunoprecipitation analysis, cells expressing epitope-tagged proteins were lysed with HBST buffer containing protease inhibitor cocktail (Roche). Cell lysates were immunoprecipitated with EZview Red Affinity Gel (Sigma), and bound proteins were analyzed by Western blotting.

### Quantitative phosphatase assays

Phosphorylated or unphosphorylated Vpu peptides including $Ser^{52}$ and $Ser^{56}$ ($AEDS_{52}GNES_{56}EGE$) were chemically synthesized by Scrum Inc. Cells in six-well plates were transfected with pCMV-HA-SCYL2. Two days later, cell lysates were prepared with HBST buffer containing protease inhibitor cocktail alone or with 10 nM OA. Cell lysates were immunoprecipitated with an anti-HA antibody and incubated with 10 μl of 1 mM of either phosphorylated or unphosphorylated Vpu peptide in 50 μl of reaction buffer [50 mM imidazole (pH 7.2), 200 μM EGTA, 0.25% β-mercaptoethanol, BSA (0.1 mg/ml)] at 37°C for 8 hours. To stop the reactions, 50 μl of 20 mM ammonium molybdate was added to the mixture. The amounts of free phosphate ion were measured by absorbance at 630 nm. Standard curves were obtained with a Ser/Thr phosphatase assay kit (Promega) according to the manufacturer's instructions.

### Luciferase reporter assays

Cells in 24-well plates were transfected with the pGL4-based luciferase reporter plasmid and with pGL4-TK-Rluc (Promega) as a transfection control. Two days later, cells were treated with IFN-β (1000 U/ml) for 8 hours before being harvested. Luciferase activity was determined with a Dual-Luciferase Reporter assay system (Promega) and normalized to *Renilla* luciferase activity.

### Statistical analysis

All graphs present the means and SDs. Statistical significance of differences between two groups was tested by two-tailed unpaired *t* test with Prism 6 software (GraphPad). In cases where multiple comparisons within an experiment were made, one-way analysis of variance (ANOVA) was used. A $P$ value of $<0.05$ was considered statistically significant.

### SUPPLEMENTARY MATERIALS

www.sciencesignaling.org/cgi/content/full/5/245/ra73/DC1

Fig. S1. Schematic representation of the initial screening method.
Fig. S2. The CKII inhibitor DRB phenocopies the effect of increased SCYL2 abundance.
Fig. S3. SCYL2 fails to inhibit $SIV_{GSN}$ Vpu–induced counteraction of BST2.
Fig. S4. SCYL2 inhibits Vpu function through a phosphorylation-dependent mechanism.

### REFERENCES AND NOTES

1. M. H. Malim, M. Emerman, HIV-1 accessory proteins—Ensuring viral survival in a hostile environment. *Cell Host Microbe* **3**, 388–398 (2008).
2. P. D. Bieniasz, The cell biology of HIV-1 virion genesis. *Cell Host Microbe* **5**, 550–558 (2009).
3. N. J. Arhel, F. Kirchhoff, Implications of Nef: Host cell interactions in viral persistence and progression to AIDS. *Curr. Top. Microbiol. Immunol.* **339**, 147–175 (2009).
4. F. Kirchhoff, Immune evasion and counteraction of restriction factors by HIV-1 and other primate lentiviruses. *Cell Host Microbe* **8**, 55–67 (2010).

5. J. Guatelli, How innate immunity can inhibit the release of HIV-1 from infected cells. *N. Engl. J. Med.* **362**, 553–554 (2010).
6. K. Strebel, T. Klimkait, M. A. Martin, A novel gene of HIV-1, vpu, and its 16-kilodalton product. *Science* **241**, 1221–1223 (1988).
7. E. A. Cohen, E. F. Terwilliger, J. G. Sodroski, W. A. Haseltine, Identification of a protein encoded by the *vpu* gene of HIV-1. *Nature* **334**, 532–534 (1988).
8. T. Huet, R. Cheynier, A. Meyerhans, G. Roelants, S. Wain-Hobson, Genetic organization of a chimpanzee lentivirus related to HIV-1. *Nature* **345**, 356–359 (1990).
9. R. L. Willey, F. Maldarelli, M. A. Martin, K. Strebel, Human immunodeficiency virus type 1 Vpu protein induces rapid degradation of CD4. *J. Virol.* **66**, 7193–7200 (1992).
10. S. J. Neil, T. Zang, P. D. Bieniasz, Tetherin inhibits retrovirus release and is antagonized by HIV-1 Vpu. *Nature* **451**, 425–430 (2008).
11. N. Van Damme, D. Goff, C. Katsura, R. L. Jorgenson, R. Mitchell, M. C. Johnson, E. B. Stephens, J. Guatelli, The interferon-induced protein BST-2 restricts HIV-1 release and is downregulated from the cell surface by the viral Vpu protein. *Cell Host Microbe* **3**, 245–252 (2008).
12. S. Bour, C. Perrin, K. Strebel, Cell surface CD4 inhibits HIV-1 particle release by interfering with Vpu activity. *J. Biol. Chem.* **274**, 33800–33806 (1999).
13. J. Lama, A. Mangasarian, D. Trono, Cell-surface expression of CD4 reduces HIV-1 infectivity by blocking Env incorporation in a Nef- and Vpu-inhibitable manner. *Curr. Biol.* **9**, 622–631 (1999).
14. R. L. Willey, F. Maldarelli, M. A. Martin, K. Strebel, Human immunodeficiency virus type 1 Vpu protein regulates the formation of intracellular gp160-CD4 complexes. *J. Virol.* **66**, 226–234 (1992).
15. J. L. Douglas, K. Viswanathan, M. N. McCarroll, J. K. Gustin, K. Früh, A. V. Moses, Vpu directs the degradation of the human immunodeficiency virus restriction factor BST-2/Tetherin via a βTrCP-dependent mechanism. *J. Virol.* **83**, 7931–7947 (2009).
16. E. Miyagi, A. J. Andrew, S. Kao, K. Strebel, Vpu enhances HIV-1 virus release in the absence of Bst-2 cell surface down-modulation and intracellular depletion. *Proc. Natl. Acad. Sci. U.S.A.* **106**, 2868–2873 (2009).
17. C. Goffinet, I. Allespach, S. Homann, H. M. Tervo, A. Habermann, D. Rupp, L. Oberbremer, C. Kern, N. Tibroni, S. Welsch, J. Krijnse-Locker, G. Banting, H. G. Kräusslich, O. T. Fackler, O. T. Keppler, HIV-1 antagonism of CD317 is species specific and involves Vpu-mediated proteasomal degradation of the restriction factor. *Cell Host Microbe* **5**, 285–297 (2009).
18. K. Sato, S. P. Yamamoto, N. Misawa, T. Yoshida, T. Miyazawa, Y. Koyanagi, Comparative study on the effect of human BST-2/Tetherin on HIV-1 release in cells of various species. *Retrovirology* **6**, 53 (2009).
19. Y. Iwabu, H. Fujita, M. Kinomoto, K. Kaneko, Y. Ishizaka, Y. Tanaka, T. Sata, K. Tokunaga, HIV-1 accessory protein Vpu internalizes cell-surface BST-2/tetherin through transmembrane interactions leading to lysosomes. *J. Biol. Chem.* **284**, 35060–35072 (2009).
20. H. Hauser, L. A. Lopez, S. J. Yang, J. E. Oldenburg, C. M. Exline, J. C. Guatelli, P. M. Cannon, HIV-1 Vpu and HIV-2 Env counteract BST-2/tetherin by sequestration in a perinuclear compartment. *Retrovirology* **7**, 51 (2010).
21. M. Skasko, Y. Wang, Y. Tian, A. Tokarev, J. Munguia, A. Ruiz, E. B. Stephens, S. J. Opella, J. Guatelli, HIV-1 Vpu protein antagonizes innate restriction factor BST-2 via lipid-embedded helix-helix interactions. *J. Biol. Chem.* **287**, 58–67 (2012).
22. E. Bartee, A. McCormack, K. Früh, Quantitative membrane proteomics reveals new cellular targets of viral immune modulators. *PLoS Pathog.* **2**, e107 (2006).
23. B. Mangeat, G. Gers-Huber, M. Lehmann, M. Zufferey, J. Luban, V. Piguet, HIV-1 Vpu neutralizes the antiviral factor Tetherin/BST-2 by binding it and directing its β-TrCP2-dependent degradation. *PLoS Pathog.* **5**, e1000574 (2009).
24. R. S. Mitchell, C. Katsura, M. A. Skasko, K. Fitzpatrick, D. Lau, A. Ruiz, E. B. Stephens, F. Margottin-Goguet, R. Benarous, J. C. Guatelli, Vpu antagonizes BST-2–mediated restriction of HIV-1 release via β-TrCP and endo-lysosomal trafficking. *PLoS Pathog.* **5**, e1000450 (2009).
25. R. K. Gupta, S. Hué, T. Schaller, E. Verschoor, D. Pillay, G. J. Towers, Mutation of a single residue renders human tetherin resistant to HIV-1 Vpu-mediated depletion. *PLoS Pathog.* **5**, e1000443 (2009).
26. D. Perez-Caballero, T. Zang, A. Ebrahimi, M. W. McNatt, D. A. Gregory, M. C. Johnson, P. D. Bieniasz, Tetherin inhibits HIV-1 release by directly tethering virions to cells. *Cell* **139**, 499–511 (2009).
27. K. Fitzpatrick, M. Skasko, T. J. Deerinck, J. Crum, M. H. Ellisman, J. Guatelli, Direct restriction of virus release and incorporation of the interferon-induced protein BST-2 into HIV-1 particles. *PLoS Pathog.* **6**, e1000701 (2010).
28. J. Hammonds, J. J. Wang, H. Yi, P. Spearman, Immunoelectron microscopic evidence for Tetherin/BST2 as the physical bridge between HIV-1 virions and the plasma membrane. *PLoS Pathog.* **6**, e1000749 (2010).
29. U. Schubert, T. Schneider, P. Henklein, K. Hoffmann, E. Berthold, H. Hauser, G. Pauli, T. Porstmann, Human-immunodeficiency-virus-type-1-encoded Vpu protein is phosphorylated by casein kinase II. *Eur. J. Biochem.* **204**, 875–883 (1992).
30. U. Schubert, K. Strebel, Differential activities of the human immunodeficiency virus type 1-encoded Vpu protein are regulated by phosphorylation and occur in different cellular compartments. *J. Virol.* **68**, 2260–2271 (1994).
31. F. Margottin, S. P. Bour, H. Durand, L. Selig, S. Benichou, V. Richard, D. Thomas, K. Strebel, R. Benarous, A novel human WD protein, h-βTrCp, that interacts with HIV-1 Vpu connects CD4 to the ER degradation pathway through an F-box motif. *Mol. Cell* **1**, 565–574 (1998).
32. C. Butticaz, O. Michielin, J. Wyniger, A. Telenti, S. Rothenberger, Silencing of both β-TrCP1 and HOS (β-TrCP2) is required to suppress human immunodeficiency virus type 1 Vpu-mediated CD4 down-modulation. *J. Virol.* **81**, 1502–1505 (2007).
33. A. A. Tokarev, J. Munguia, J. C. Guatelli, Serine-threonine ubiquitination mediates downregulation of BST-2/tetherin and relief of restricted virion release by HIV-1 Vpu. *J. Virol.* **85**, 51–63 (2011).
34. R. Vigan, S. J. Neil, Determinants of tetherin antagonism in the transmembrane domain of the human immunodeficiency virus type 1 Vpu protein. *J. Virol.* **84**, 12958–12970 (2010).
35. C. F. Basler, A. Garcia-Sastre, Viruses and the type I interferon antiviral system: Induction and evasion. *Int. Rev. Immunol.* **21**, 305–337 (2002).
36. C. E. Samuel, Antiviral actions of interferons. *Clin. Microbiol. Rev.* **14**, 778–809 (2001).
37. M. J. de Veer, M. Holko, M. Frevel, E. Walker, S. Der, J. M. Paranjape, R. H. Silverman, B. R. Williams, Functional classification of interferon-stimulated genes identified using microarrays. *J. Leukoc. Biol.* **69**, 912–920 (2001).
38. A. L. Blasius, E. Giurisato, M. Cella, R. D. Schreiber, A. S. Shaw, M. Colonna, Bone marrow stromal cell antigen 2 is a specific marker of type I IFN-producing cells in the naive mouse, but a promiscuous cell surface antigen following IFN stimulation. *J. Immunol.* **177**, 3260–3265 (2006).
39. G. Poli, J. M. Orenstein, A. Kinter, T. M. Folks, A. S. Fauci, Interferon-alpha but not AZT suppresses HIV expression in chronically infected cell lines. *Science* **244**, 575–577 (1989).
40. A. Okumura, G. Lu, I. Pitha-Rowe, P. M. Pitha, Innate antiviral response targets HIV-1 release by the induction of ubiquitin-like protein ISG15. *Proc. Natl. Acad. Sci. U.S.A.* **103**, 1440–1445 (2006).
41. S. D. Barr, J. R. Smiley, F. D. Bushman, The interferon response inhibits HIV particle production by induction of TRIM22. *PLoS Pathog.* **4**, e1000007 (2008).
42. T. Sawasaki, T. Ogasawara, R. Morishita, Y. Endo, A cell-free protein synthesis system for high-throughput proteomics. *Proc. Natl. Acad. Sci. U.S.A.* **99**, 14652–14657 (2002).
43. E. F. Ullman, H. Kirakossian, S. Singh, Z. P. Wu, B. R. Irvin, J. S. Pease, A. C. Switchenko, J. D. Irvine, A. Dafforn, C. N. Skold, D. B. Wagner, Luminescent oxygen channeling immunoassay: Measurement of particle binding kinetics by chemiluminescence. *Proc. Natl. Acad. Sci. U.S.A.* **91**, 5426–5430 (1994).
44. A. Von Leoprechting, R. Kumpf, S. Menzel, D. Reulle, R. Griebel, M. J. Valler, F. H. Büttner, Miniaturization and validation of a high-throughput serine kinase assay using the AlphaScreen platform. *J. Biomol. Screen.* **9**, 719–725 (2004).
45. M. Mansouri, K. Viswanathan, J. L. Douglas, J. Hines, J. Gustin, A. V. Moses, K. Früh, Molecular mechanism of BST2/tetherin downregulation by K5/MIR2 of Kaposi's sarcoma-associated herpesvirus. *J. Virol.* **83**, 9672–9681 (2009).
46. C. Pardieu, R. Vigan, S. J. Wilson, A. Calvi, T. Zang, P. Bieniasz, P. Kellam, G. J. Towers, S. J. Neil, The RING-CH ligase K5 antagonizes restriction of KSHV and HIV-1 particle release by mediating ubiquitin-dependent endosomal degradation of tetherin. *PLoS Pathog.* **6**, e1000843 (2010).
47. E. Kinoshita, M. Takahashi, H. Takeda, M. Shiro, T. Koike, Recognition of phosphate monoester dianion by an alkoxide-bridged dinuclear zinc(II) complex. *Dalton Trans.* **8**, 1189–1193 (2004).
48. E. Kinoshita, E. Kinoshita-Kikuta, K. Takiyama, T. Koike, Phosphate-binding tag, a new tool to visualize phosphorylated proteins. *Mol. Cell. Proteomics* **5**, 749–757 (2006).
49. E. Kinoshita, E. Kinoshita-Kikuta, T. Koike, Separation and detection of large phosphoproteins using Phos-tag SDS-PAGE. *Nat. Protoc.* **4**, 1513–1521 (2009).
50. S. D. Conner, S. L. Schmid, CVAK104 is a novel poly-L-lysine-stimulated kinase that targets the β2-subunit of AP2. *J. Biol. Chem.* **280**, 21539–21544 (2005).
51. M. Düwel, E. J. Ungewickell, Clathrin-dependent association of CVAK104 with endosomes and the *trans*-Golgi network. *Mol. Biol. Cell* **17**, 4513–4525 (2006).
52. G. H. Borner, A. A. Rana, R. Forster, M. Harbour, J. C. Smith, M. S. Robinson, CVAK104 is a novel regulator of clathrin-mediated SNARE sorting. *Traffic* **8**, 893–903 (2007).
53. V. Janssens, J. Goris, C. Van Hoof, PP2A: The expected tumor suppressor. *Curr. Opin. Genet. Dev.* **15**, 34–41 (2005).
54. M. Dubé, B. B. Roy, P. Guiot-Guillain, J. Binette, J. Mercier, A. Chiasson, E. A. Cohen, Antagonism of tetherin restriction of HIV-1 release by Vpu involves binding and sequestration of the restriction factor in a perinuclear compartment. *PLoS. Pathog.* **6**, e1000856 (2010).
55. H. M. Tervo, S. Homann, I. Ambiel, J. V. Fritz, O. T. Fackler, O. T. Keppler, β-TrCP is dispensable for Vpu's ability to overcome the CD317/Tetherin-imposed restriction to HIV-1 release. *Retrovirology* **8**, 9 (2011).
56. T. K. Kerppola, Design and implementation of bimolecular fluorescence complementation (BiFC) assays for the visualization of protein interactions in living cells. *Nat. Protoc.* **1**, 1278–1286 (2006).
57. T. Kobayashi, H. Ode, T. Yoshida, K. Sato, P. Gee, S. P. Yamamoto, H. Ebina, K. Strebel, H. Sato, Y. Koyanagi, Identification of amino acids in the human tetherin transmembrane

domain responsible for HIV-1 Vpu interaction and susceptibility. *J. Virol.* **85**, 932–945 (2011).
58. R. A. Liberatore, P. D. Bieniasz, Tetherin is a key effector of the antiretroviral activity of type I interferon in vitro and in vivo. *Proc. Natl. Acad. Sci. U.S.A.* **108**, 18097–18101 (2011).
59. T. Terabayashi, Y. Funato, M. Fukuda, H. Miki, A coated vesicle-associated kinase of 104 kDa (CVAK104) induces lysosomal degradation of frizzled 5 (Fzd5). *J. Biol. Chem.* **284**, 26716–26724 (2009).
60. D. Schwartz, G. M. Church, Collection and motif-based prediction of phosphorylation sites in human viruses. *Sci. Signal.* **3**, rs2 (2010).
61. A. G. Bukrinskaya, A. Ghorpade, N. K. Heinzinger, T. E. Smithgall, R. E. Lewis, M. Stevenson, Phosphorylation-dependent human immunodeficiency virus type 1 infection and nuclear targeting of viral DNA. *Proc. Natl. Acad. Sci. U.S.A.* **93**, 367–371 (1996).
62. L. A. Pinna, Protein kinase CK2: A challenge to canons. *J. Cell Sci.* **115**, 3873–3878 (2002).
63. M. C. Mumby, G. Walter, Protein serine/threonine phosphatases: Structure, regulation, and functions in cell growth. *Physiol. Rev.* **73**, 673–699 (1993).
64. V. Janssens, J. Goris, Protein phosphatase 2A: A highly regulated family of serine/threonine phosphatases implicated in cell growth and signalling. *Biochem. J.* **353**, 417–439 (2001).
65. K. Okamoto, H. Li, M. R. Jensen, T. Zhang, Y. Taya, S. S. Thorgeirsson, C. Prives, Cyclin G recruits PP2A to dephosphorylate Mdm2. *Mol. Cell* **9**, 761–771 (2002).
66. D. Lau, W. Kwan, J. Guatelli, Role of the endocytic pathway in the counteraction of BST-2 by human lentiviral pathogens. *J. Virol.* **85**, 9834–9846 (2011).
67. T. Kueck, S. J. Neil, A cytoplasmic tail determinant in HIV-1 Vpu mediates targeting of tetherin for endosomal degradation and counteracts interferon-induced restriction. *PLoS Pathog.* **8**, e1002609 (2012).
68. N. Belaïdouni, C. Marchal, R. Benarous, C. Besnard-Guérin, Involvement of the βTrCP in the ubiquitination and stability of the HIV-1 Vpu protein. *Biochem. Biophys. Res. Commun.* **357**, 688–693 (2007).
69. D. Tadokoro, S. Takahama, K. Shimizu, S. Hayashi, Y. Endo, T. Sawasaki, Characterization of a caspase-3-substrate kinome using an N- and C-terminally tagged protein kinase library produced by a cell-free system. *Cell Death Dis.* **1**, e89 (2010).
70. T. Sawasaki, R. Morishita, M. D. Gouda, Y. Endo, Methods for high-throughput materialization of genetic information based on wheat germ cell-free expression system. *Methods Mol. Biol.* **375**, 95–106 (2007).
71. K. Takai, T. Sawasaki, Y. Endo, Practical cell-free protein synthesis system using purified wheat embryos. *Nat. Protoc.* **5**, 227–238 (2010).
72. A. Adachi, H. E. Gendelman, S. Koenig, T. Folks, R. Willey, A. Rabson, M. A. Martin, Production of acquired immunodeficiency syndrome-associated retrovirus in human and nonhuman cells transfected with an infectious molecular clone. *J. Virol.* **59**, 284–291 (1986).
73. K. L. Nguyen, M. Ilano, H. Akari, E. Miyagi, E. M. Poeschla, K. Strebel, S. Bour, Codon optimization of the HIV-1 *vpu* and *vif* genes stabilizes their mRNA and allows for highly efficient Rev-independent expression. *Virology* **319**, 163–175 (2004).
74. T. Klimkait, K. Strebel, M. D. Hoggan, M. A. Martin, J. M. Orenstein, The human immunodeficiency virus type 1-specific protein vpu is required for efficient virus maturation and release. *J. Virol.* **64**, 621–629 (1990).
75. R. E. Means, S. M. Lang, J. U. Jung, The Kaposi's sarcoma-associated herpesvirus K5 E3 ubiquitin ligase modulates targets by multiple molecular mechanisms. *J. Virol.* **81**, 6573–6583 (2007).
76. T. Ohnishi, A. Yamashita, I. Kashima, T. Schell, K. R. Anders, A. Grimson, T. Hachiya, M. W. Hentze, P. Anderson, S. Ohno, Phosphorylation of hUPF1 induces formation of mRNA surveillance complexes containing hSMG-5 and hSMG-7. *Mol. Cell* **12**, 1187–1200 (2003).
77. K. Miyakawa, A. Ryo, T. Murakami, K. Ohba, S. Yamaoka, M. Fukuda, J. Guatelli, N. Yamamoto, BCA2/Rabring7 promotes tetherin-dependent HIV-1 restriction. *PLoS Pathog.* **5**, e1000700 (2009).

**Acknowledgments:** We thank K. Strebel (NIH), P. Cannon (University of Southern California), and Chugai Pharmaceutical Co. for various reagents. We also thank all members of the Ryo laboratory for technical support and useful suggestions. **Funding:** This work was in part supported by a research grant from the Ministry of Health, Labour, and Welfare, Japan; a grant from Special Coordination Funds for Promoting Science and Technology; grants from Takeda Science Foundation and Uehara Memorial Foundation to A.R.; National University of Singapore School of Medicine Start-up Grant (R-182-000-160-733, R-182-000-160-133); a grant from the National Medical Research Council, Singapore (NMRC/R-182-000-182-213) to N.Y.; and a grant from the NIH (AI081668) to J.G. **Author contributions:** K.M. designed and performed the research, analyzed the data, and wrote the manuscript; T.S. developed the screening system; S.M. and A.T. performed the research; G.Q., H.K., and N.Y. analyzed the data and edited the manuscript; M.N. and A.A. contributed reagents and analyzed the data; J.G. analyzed the data and edited the manuscript; and A.R. directed the research, analyzed the data, and wrote the manuscript. **Competing interests:** The authors declare that they have no competing interests.

Submitted 11 May 2012
Accepted 20 September 2012
Final Publication 9 October 2012
10.1126/scisignal.2003212
**Citation:** K. Miyakawa, T. Sawasaki, S. Matsunaga, A. Tokarev, G. Quinn, H. Kimura, M. Nomaguchi, A. Adachi, N. Yamamoto, J. Guatelli, A. Ryo, Interferon-induced SCYL2 limits release of HIV-1 by triggering PP2A-mediated dephosphorylation of the viral protein Vpu. *Sci. Signal.* **5**, ra73 (2012).

JOURNAL OF PROTEOMICS 75 (2012) 1863–1873

Available online at www.sciencedirect.com

SciVerse ScienceDirect

www.elsevier.com/locate/jprot

# Molecular and enzymatic characterization of XMRV protease by a cell-free proteolytic analysis

*Satoko Matsunaga*[a], *Tatsuya Sawasaki*[b], *Hirotaka Ode*[c], *Ryo Morishita*[a,d], *Ayako Furukawa*[e], *Ryuta Sakuma*[f], *Wataru Sugiura*[c], *Hironori Sato*[g], *Masato Katahira*[e], *Akifumi Takaori-Kondo*[h], *Naoki Yamamoto*[i], *Akihide Ryo*[a,*]

[a]*Department of Microbiology, Yokohama City University School of Medicine, Yokohama 236-0004, Japan*
[b]*Cell-Free Science and Technology Research Center, Ehime University, Matsuyama 790-8577, Japan*
[c]*Clinical Research Center, National Hospital Organization Nagoya Medical Center, Nagoya 460-0001, Japan*
[d]*CellFree Sciences Co., Ltd., Ehime Univ. Venture Business Laboratory, Matsuyama 790-8577, Japan*
[e]*Institute of Advanced Energy, Kyoto University, Kyoto 611-0011, Japan*
[f]*Department of Molecular Virology, Tokyo Medical and Dental University, Tokyo 113-8510, Japan*
[g]*Pathogen Genomics Center, National Institutes of Infectious Diseases, Tokyo 208-0011, Japan*
[h]*Department of Hematology and Oncology, Graduate School of Medicine, Kyoto University, Kyoto 606-8507, Japan*
[i]*Department of Microbiology, National University of Singapore, Singapore 117597, Singapore*

ARTICLE INFO

*Article history:*
Received 21 March 2012
Accepted 31 May 2012
Available online 9 June 2012

*Keywords:*
XMRV
Protease
Cell-free protein synthesis
AlphaSceen

ABSTRACT

Xenotropic murine leukemia virus-related virus (XMRV) is a virus generated under artificial conditions by the recombination of 2 murine leukemia virus (MLV) proviruses, PreXMRV-1 and PreXMRV-2, during the in vivo passage of human prostate cancer cells in athymic nude mice. The molecular etiology of XMRV infection has not been characterized and its implication in human prostate cancer progression remains equivocal. As a step toward resolving this issue we developed an in vitro enzymatic assay system to characterize XMRV protease (PR)-mediated cleavage of host-cell proteins. Enzymatically-active XMRV PR protein was synthesized using a wheat-germ cell-free system. By monitoring cleavage activity of XMRV PR by AlphaScreen and 2-color immunoblot analyses, we revealed that the catalytic activity of XMRV PR is selectively blocked by the HIV PR inhibitor, Amprenavir, and identified several human tumor suppressor proteins, including PTEN and BAX, to be substrates of XMRV PR. This system may provide an attractive means for analyzing the function of retrovirus proteases and provide a technology platform for drug screening.



## 1. Introduction

Xenotropic murine leukemia virus-related virus (XMRV) was originally isolated from a human prostate cancer (PC) in 2006 [1]. This virus is highly homologous to several endogenous Murine leukemia viruses (MLVs) found in mice [2]. Although previous reports suggested the involvement of XMRV in PC as well as chronic fatigue syndrome (CFS), as an etiological agent, no evidence of this etiological link between XMRV and human disease has been shown to date [3–5].

The nucleotide sequence of XMRV isolated from humans indicates that the virus is nearly identical with the XMRV isolated from the human prostate tumor cell line 22Rv1 [6]. This cell line was generated by serial passage of human prostate tumor tissue in nude mice. Sequence analysis revealed that the genomes of these mouse strains contain two different proviral

* *Corresponding author.* Tel.: +81 45 787 2602; fax: +81 45 787 2851.
E-mail address: aryo@yokohama-cu.ac.jp (A. Ryo).

1874-3919/$ – see front matter © 2012 Elsevier B.V. All rights reserved.
doi:10.1016/j.jprot.2012.05.047

DNAs related to XMRV (Pre-XMRV-1 and 2). It appears that these proviral genomes recombined to produce the XMRV isolated from 22Rv1 cells. It is plausible that the reported association of XMRV with human disease is due to contamination of human samples with virus originating from this recombination event in mice prior to the analysis.

While XMRV arose from an unusual recombination, several lines of study have indicated that XMRV can indeed infect, and proliferate in, several human prostate cancer cell lines including LNCaP and PC3 [7]. It is of significance that dihydrotestosterone (DHT) was shown to stimulate transcription and replication of XMRV through the transactivation of the XMRV-LTR via the hormone response element (HRE) [8]. Mutations in the HRE of XMRV impaired basal transcription and androgen responsiveness, suggesting a relationship between virus productivity and prostatic hypertrophy and neoplasia.

If XMRV is indeed an etiological agent in PCs, detection and elimination of XMRV infection could provide an effective strategy for early diagnosis and treatment of this tumor. To date, however, conflicting epidemiological data has precluded investigations into whether the virus is truly pathogenic or not and, moreover, whether this virus is oncogenic and associated with human PCs.

Retroviral protease (PR) is essential for virus replication and has been the major target for anti-retroviral therapy. Concomitant with particle release, the virally-encoded PR cleaves Gag into its four mature protein domains; MA, CA, NC and p12, in case of XMRV. Gag-Pol is also cleaved by PR, creating the viral enzymes RT, IN and PR itself. The maturation step coupled with PR activation is essential to confer viral infectivity. Therefore, for the effective inhibition of XMRV infection, should this virus be found to be pathogenic, development of anti-retroviral drugs targeting the XMRV protease would seem logical.

Several recent studies have indicated that viral-protease cleavage of host proteins that promotes viral replication and cytopathic effects [9–11]. It remains elusive whether this is the case for XMRV PR. One of the major bottlenecks in PR research has been the difficulty in producing recombinant protein with enzymatic activity in conventional cell-associated protein expression systems (e.g. *E. coli* or insect cell) due to host cell toxicity.

The wheat germ protein production system is a robust in vitro cell-free protein synthesis system comprising a crude wheat germ extract containing ions (buffer) and all the macromolecular components required for protein translation (e.g. ribosomes, tRNAs, aminoacyl-tRNA synthetases, initiation, elongation and termination factors) [12,13]. The extract is further supplemented with amino acids, energy sources such as ATP, energy generating systems and cofactors for efficient and abundant protein production. This system is a powerful tool for the preparation of multiple proteins at one time, and large amounts of specific proteins for both biochemical and biomedical applications. It also enables synthesis of specific proteins that are difficult to express and/or purify in *E. coli* or other cell-based systems. The wheat germ system can produce a wide variety of proteins, including viral proteins, in sufficient amounts for functional assays. Furthermore, this system can yield enzymatically-active proteins in their naturally folded state owing to the constituent eukaryotic translation and folding machinery.

In our current study, we utilized the wheat germ cell-free system to synthesize catalytically active XMRV PR for the identification of potential inhibitors and substrates. By this approach we delineated a molecular link between XMRV PR and human tumor suppressor proteins pointing to a potential role in oncogenesis.

## 2. Materials and methods

### 2.1. *Construction of DNA template for transcription and the protein expression*

DNA templates were made using the Gateway and split-primer polymerase chain reaction (PCR) systems [12,14,15]. The tumor suppressor genes were amplified from MGC, a human cDNA resource purchased from Danaform (Tokyo, Japan).

The XMRV protease fragment was amplified by PCR from XMRV VP62 clone [1,16] using the following forward and reverse primers, respectively: (5′-GGGGACAAGTTTGTACAAAAAAGCAGGCTTCATGAAGGACTGCCCAAAGAAGCC-3′) and (5′-GGGGACCACTTTGTACAAGAA AGCTGGGTCTTATAGAGGAACATCTGGCTC-3′). For HIV-1 protease, cDNA fragment was amplified by PCR from HIV-1 NL4-3 clone by using the following forward and reverse primers, respectively: (5′-CCACCCACCACCACCAATGTTTTTTAGGGAAGATC-3′) and (5′-TCCAGCACTAGCTCCAGATTAGCCATCCATTCCTGGC-3′). Subsequently, attB-flanked fragment were amplified by PCR using attB1-S1 primer (5′-GGGGACAAGTTTGTACAAAAAAGCAGGCTTCCACCCACCACCACCAATG-3′) and attB2-T1 primer (5′-GGGGACCACTTTGTACAAGAAAGCTGGGTCTCCAGCACTAGCTCCAGA-3′). The single Capsid (CA) and Nucleocapsid (NC) fragment of XMRV Gag (control substrate), and the 24 tumor suppressor gene fragments (test substrates) were amplified by two-step PCR (without stop codon). The first round of PCR was performed on using 10 nM of S1 (forward) primer (5′- CCACCCACCACCACCAatg(n)19-3′) and T1 (reverse) primer (5′-TCCAGCACTAGCTCCAGA(n)19-3′). The second round of PCR was carried out using the first PCR product as template, with 100nM of attB1-FLAG-S1 (forward) primer (5′-GGGGACAAGTTTGTACAAAAAAGCAGGCTTCATGGACTACAAGGATGACGATGACAAGCTCCACCCACCACCACCAATG-3′) and T1-biotin ligase site (bls)-stop-attB2-anti (reverse) primer (5′-GGGGACCACTTTGTACAAGAAAGCTGGGTTTATTCGTGCCACTCGATCTTCTGGGCCTCGAAGATGTCGTTCAGGCCGCTTCCAGCACTAGCTCCAGA-3′) [17].

The amplified attB-flanked fragments were each inserted into the pDONR221 vector using the Gateway BP Clonase II enzyme mix (Invitrogen, Carlsbad, CA, USA) to give pDONR-XMRV PR vector and pDONR-FLAG-gene-bls vectors, respectively.

pDONR-XMRV PR and pDONR-FLAG-CA/NC-bls vectors were subcloned into pEU-E01-GW [18] to generate the pEU-based-plasmids by LR reaction. BP and LR reactions were performed according to the manufacturer's instructions (Invitrogen). PCR reactions were performed using PrimeStar enzyme according to the manufacturer's instructions (Takara Bio, Otsu, Japan).

For HIV-1 PR substrate, the p2–p7 fragment in HIV-1 Gag precursor was amplified by PCR from HIV-1 NL4-3 clone by using the following forward and reverse primers, respectively: (5′-GAGACTCGAGGCCGAGGCCATGAGCCAGG-3′) and

(5′-GAGCGGTACCTTATTCGTGCCACTCGATCTTCTGGGCCTC-GAAGATGTCGTTCAGGCCATTAGCCTGCCTCTCGGTGCA-3′). The p2–p7-bls fragment was inserted into the pEU-E01-GST-MCS vector (Cellfree Sciences, Yokohama, Japan). The transcription template from pEU vector was amplified using the following forward and reverse primers, respectively: SPu primer (5′-GCGTAGCATTTAGGTGACACT-3′) and AODA2303 (5′-GTCA-GACCCCGTAGAAAAGA-3′). PCR was carried out using the TaKaRa Ex Taq (Takara Bio Inc, Shiga, Japan) according to the manufacturer's instructions.

DNA templates of human genes for transcription were constructed using split-primer PCR in two steps as described previously [18]. For the first step, S1 primers and pDONR221-1st_4080 (5′-ATCTTTTCTACGGGGTCTGA-3′) or AODA2306 (5′- AGCGTCAGACCCCGTAGAAA -3′) were used. For the second step, the primers SPu and pDONR221-2nd_4035 (5′-ACGTTAAGG-GATTTTGGTCA-3′) or AODA2303 were used to generate the final DNA template for transcription.

### 2.2. Cell-free protein synthesis

In vitro transcription and cell-free protein synthesis was performed as described previously [19]. Transcripts were made from each of the DNA templates mentioned above using SP6 RNA polymerase. The synthetic mRNAs were then precipitated with ethanol, collected by centrifugation and washed. Each mRNA (typically 30–35 μg) was added to the translation mixture and the translation reaction was performed in the bilayer mode [20] with slight modifications. The translation mixture that formed the bottom layer consisted of 60 A260 units of wheat germ extract (CellFree Sciences) and 2 μg creatine kinase (Roche Diagnostics K. K., Tokyo, Japan) in 25 μl SUB-AMIX solution (CellFree Sciences). SUB-AMIX contained (final concentrations) 30 mM Hepes/KOH at pH 8.0, 1.2 mM ATP, 0.25 mM GTP, 16 mM creatine phosphate, 4 mM DTT, 0.4 mM spermidine, 0.3 mM each of the 20 amino acids, 2.7 mM magnesium acetate, and 100 mM potassium acetate. SUB-AMIX (125 μl) was placed on the top of the translation mixture, forming the upper layer. After incubation at 16 °C for 16 h, protein synthesis was confirmed by SDS-PAGE. For biotin labeling, 1 μl (50 ng) of crude biotin ligase (BirA) produced by the wheat germ cell-free expression system was added to the bottom layer, and 0.5 μM (final concentration) of D-biotin (Nacalai Tesque, Inc., Kyoto, Japan) was added to both upper and bottom layers, as described previously [21].

### 2.3. Detection of cleavage activity of XMRV protease by luminometry

In vitro cleavage activity assays of XMRV protease were carried out in a total volume of 15 μl consisting of 100 mM Tris–HCl pH 8.0, 0.01% Tween-20, 1 mg/ml BSA, 1 μl crude recombinant protease (~0.75 μM) and 0.5 μl crude recombinant FLAG-biotin-tagged CA/NC (~0.037 μM) at 37 °C for 1 h in a 384-well Optiplate (PerkinElmer, Boston, MA, USA). To assay the effects of HIV protease inhibitors on XMRV protease, after 3 μl recombinant viral protease and HIV protease inhibitor was incubated at 37 °C for 10 min, FLAG-biotin-tagged CA/NC or GST-biotin-tagged p2–p7 was added and the reaction further incubated at 37 °C for 1 h in a 384-well Optiplate. In accordance with the AlphaScreen IgG (Protein A) detection kit (PerkinElmer) instruction manual, 10 μl of detection mixture containing 100 mM Tris–HCl pH 8.0, 0.01% Tween-20, 1 mg/ml BSA, 5 μg/ml Anti-FLAG antibody (Sigma-Aldrich, St. Louis, MO, USA) or Anti-GST antibody (GE Healthcare, Buckinghamshire, UK), 0.1 μl streptavidin-coated donor beads and 0.1 μl anti-IgG (Protein A) acceptor beads were added to each well followed by incubation at 26 °C for 1 h. Luminescence was analyzed by the AlphaScreen detection program. Each assay was performed in triplicate, and the data represent the means and standard deviations of three independent experiments.

### 2.4. Detection of cleavage activity by immunoblotting

3 μl crude recombinant viral protease (~0.75 μM) and 7 μl crude FLAG-biotin-tagged recombinant proteins were incubated at 37 °C for 2 h. To assay the effect of HIV protease inhibitors, 3 μl crude recombinant XMRV protease and 1 μl of 10 μM HIV protease inhibitor were incubated at 37 °C for 10 min followed by addition of 6 μl crude FLAG-biotin-tagged recombinant proteins, and incubated at 37 °C for 120 min. Proteins were separated by SDS-PAGE and transferred to a PVDF membrane (Millipore Bedford, MA, USA) according to standard procedures. Immunoblot analysis was carried out with anti-FLAG (M2) antibodies (Sigma-Aldrich) or Streptavidin-HRP conjugate (GE Healthcare) according to the procedure described above. For fluorescent imaging, immunoblotted proteins were detected by Alexa592-anti-mouse antibodies (N-cleaved fragments), and Alexa488-streptavidin (C-cleaved fragments). The labeled proteins were visualized using a Typhoon Imager (GE Healthcare).

### 2.5. Homology modeling of XMRV PR in complex with APV

To predict interactions between XMRV PR and APV, we performed homology modeling [22] of the complex structure formed between XMRV PR and APV using the Molecular Operating Environment (MOE) software ver. 2008.10. (Chemical Computing Group, Canada). Firstly, the homologues of XMRV PR were searched for with the MOE-search PDB module from the MOE homology databank. Secondly, to minimize misalignments of the target sequence, multiple alignments were made using sequences of the homologues and those of HIV-1 PR (PDB code: 1HPV) and HTLV PR (PDB code: 3LIN) with the MOE-Align module. The aligned sequences showed that amino acids at the active site of HIV-1, HTLV PRs and those likely to be at the active site of XMRV PR were comparatively conserved, suggesting a structure of HIV-1 PR with APV (PDB code: 1HPV) would be appropriate for a template structure to predict interactions between XMRV PR and APV. Thirdly, homology modeling was performed with MOE-Homology, using the structure of HIV-1 PR in complex with APV (PDB code: 1HPV) as a template structure. During the modeling, the MMFF94x force field and the GB/VI implicit solvent function [23] were applied for energy calculation. In this study, we predicted ten structures of the complex, and selected the structure with the lowest energy as the model for the XMRV PR-APV complex.

## 3. Results

### 3.1. Synthesis of an enzymatically active XMRV PR using the wheat germ cell-free system

To synthesize enzymatically-active XMRV PR, we generated a transcription template of this enzyme derived from the XMRV VP62 clone. The template cDNA encodes the open reading frame of XMRV PR flanked by N-terminal 20 amino acid and a C-terminal 20 amino acid regions, as shown in Fig. 1A (PR; 20aa-PR-20aa). This PR differs from the synthesized inactive native PR template by an introduced substitution of the termination codon at the 3′-terminus of the Gag coding sequence for Glu-coding codon (CAG) to avoid translational termination at the end of Gag protein. As a catalytic-incompetent PR, we also designed a PR mutant harboring the catalytic active site substitution D32N (PR_D32N) (Fig. 1A). All 3 cDNA templates were subjected to cell-free transcription-translation. The protein yield of XMRV PR produced by this system was approximately 0.75 μM and the solubility was ~90%, as calculated by semi-quantitative CBB staining following SDS-PAGE (Fig. 1B). By immunoblotting (IB), two specific protein bands appeared at 14 kDa and 17 kDa, corresponding to the expected mobility of the full-length PR and the truncated form of PR by auto-cleavage of the flanking 20 a.a. at both ends (Fig. 1B). The auto-cleavage site of the XMRV PR was also confirmed by amino acid sequencing of the truncated protein band (Fig. 1C).

We next examined the enzymatic activity of the XMRV PR by monitoring its cleavage activity upon a native FLAG-pr55$^{Gag}$ protein substrate. Wheat germ-synthesized XMRV PR was incubated with FLAG-pr55$^{Gag}$ protein followed by immunoblotting analysis. p55$^{Gag}$ was efficiently digested into the expected cleavage products (FLAG-MA-p12 and FLAG-MA) predicted from the known cleavage sites (Fig. 1D).

### 3.2. Evaluation of protease activity using AlphaScreen

For the quantitative and high-throughput measurement of XMRV PR activity using AlphaScreen technology, we designed a reporter substrate comprising a partial capsid (CA)-nucleo capsid (NC) junction peptide flanked by N-terminal FLAG and C-terminal biotin binding sequence (FLAG-CA/NC-biotin), as described in Materials and methods [14,15]. Fig. 2A shows a schematic representation of our assay system. Briefly, cell-free synthesized active XMRV PR, its D32N mutant or dihydrofolate reductase (DHFR) as a negative control, were incubated with the reporter substrate at 37 °C for 1 h, followed by the addition of AlphaScreen streptavidin donor and protein A acceptor beads as depicted in Fig. 2A. The cleavage of the reporter substrate was measured by level of luminescence (Fig. 2A). Wild-type XMRV PR, but not D32N_PR diminished the Alphascreen luminescent signal indicating proteolytic cleavage of the reporter polypeptide (Fig. 2B). The cleavage activity of PR was normalized relative to the luminescent activity of DHFR (Fig. 2C). Parallel immunoblot analysis with an anti-FLAG antibody demonstrated that the substrate protein was selectively cleaved by PR alone (Fig. 2D).

### 3.3. Screening of XMRV PR inhibitors by AlphaScreen

We next tested whether our assay system is applicable for drug screening targeting XMVR PR. As an initial approach, we examined the susceptibility of XMRV PR to six HIV-1 PIs: SQV (saquinavir), APV (amprenavir), IDV (indinavir), NFV (nelfinavir), DRV (darunavir) and LPV (lopinavir). Although all HIV-1 PIs tested showed marked inhibitory effects on HIV-1 PR, only two of them, APV and DRV, were found to block the activity of XMRV PR at the 1 μM concentration (Fig. 3A). This was also confirmed by IB of the blockade of cleavage of the reporter polypeptide containing the CA-NC junction (Fig. 3B). We next determined the $IC_{50}$ value by titration of PIs (Fig. 3C). For XMRV PR, the $IC_{50}$ values for APV, DRV, IDV and LPV were 0.2 μM, 1.0 μM, 60 μM and 17 μM, respectively. We next delineate the sensitivity of XMRV PR to APV in comparison with HIV-1 PR. Parallel experiment using recombinant HIV-1 PR and XMRV PR proteins revealed that $IC_{50}$ values for APV was 34.7 nM in HIV PR and 200 nM in XMRV PR, respectively (Fig. 3D). These results indicate that this assay system can provide a tool to screen for selective PR inhibitors.

Retroviruses often exhibit drug resistant properties against anti-retrovirals due to their highly frequent genomic mutation. We next asked whether our assay system is useful for investigating drug-resistant properties of XMRV PR. To predict the sites of interaction between APV and XMRV PR, we modeled the three-dimensional (3D) complex of XMRV PR bound to APV. A recently published report on the crystal structure of XMRV PR shows that XMRV PR has a structural topology similar to that of HIV-1 PR [24]. Thus, we constructed our 3D structural model of the XMRV PR-APV complex by homology modeling, using the X-ray crystal structure of the HIV-1 PR-APV complex as a starting template (Fig. 4A). The constructed model indicates that APV interacts with aspartate Asp32 of the catalytic domain of XMRV PR, and also contacts the residues Val39, Lys61, Tyr90, and Leu92. Moreover, a water molecule would intermediate interactions between APV and Ala57 of the PR. A sequence alignment of PRs between XMRV and HIV-1 shows that the Val39, Ala57, Lys61, Tyr90, and Leu92 in XMRV PR are corresponding to the Val32, Ile50, Ile54, Val82, and Ile84 in HIV-1 PR, respectively (Fig.4B). These residues in HIV-1 PR are reported to be important for interactions between HIV-1 PR and APV and associated with viral resistance against APV [25].

We then created selected site-directed mutants (V39I, K61L, A57V, V39I/A57V, Y90A/L92V) and investigated the catalytic activity and drug-resistant properties of these mutants to APV (Fig. 4C). As shown in Fig. 4C, V39I and A57V substitutions resulted in significantly ($P<0.01$) (Fig. 4C) higher drug resistance as compared with wild-type PR. This effect resulted in the 2.8-fold drug-resistance based on $IC_{50}$ value (Fig.4D). These results indicate that our current assay system can predict drug-susceptibility of mutated proteases and may be useful for drug development targeting XMRV PR.

### 3.4. Identification of human proteins cleaved by XMRV PR

As it is known that viral proteases can cleave cellular proteins [26–28], we hypothesized that XMRV PR might be capable of digesting human proteins. As a representative demonstration

we selected twenty-four tumor suppressor proteins and synthesized them with N-terminal FLAG and C-terminal biotin tags by wheat cell-free system. These tester proteins were then incubated with XMRV PR followed by 2-color immunoblot analysis (Fig.5B). The result revealed that XMRV PR, but not DHFR as a negative control, can digest 4/24 tumor suppressor proteins examined: BAX, PTEN, DKK3 and ARL11 (Fig. 5C). Cleavage of the tumor suppressor proteins by XMRV PR was clearly inhibited by APV (Fig. 5D). For BAX and PTEN, the cleavage sites by XMRV PR were determined by peptide sequencing of the C-terminal cleavage products (Fig. 5E). The cleavage sites were found to be located in functional domains of both proteins, suggesting that proteolytic digestion by XMRV PR may diminish the native function of these tumor suppressor proteins by proteolytic digestion.

Since XMRV PR and HIV-1 PR have some similarity and can both be inhibited by APV, it is highly possible that XMRV PR can cleave the same substrates as HIV-1 PR. To this end, we tested whether XMRV PR could cleave two reported HIV-1 PR substrates, caspase-8 and NDR2 [28,29]. Interestingly, XMRV PR was found to digest caspase-8 although the cleavage site was distinct from that of HIV-1 PR. In contrast, XMRV PR was not able digest NDR2. Conversely, HIV-1 PR did not cleave Bax whereas XMRV PR can cleave it. Furthermore, both proteases could not cleave p53. These results indicate that there is certain substrate specificity of retroviral proteases toward host proteins (Fig. 6).

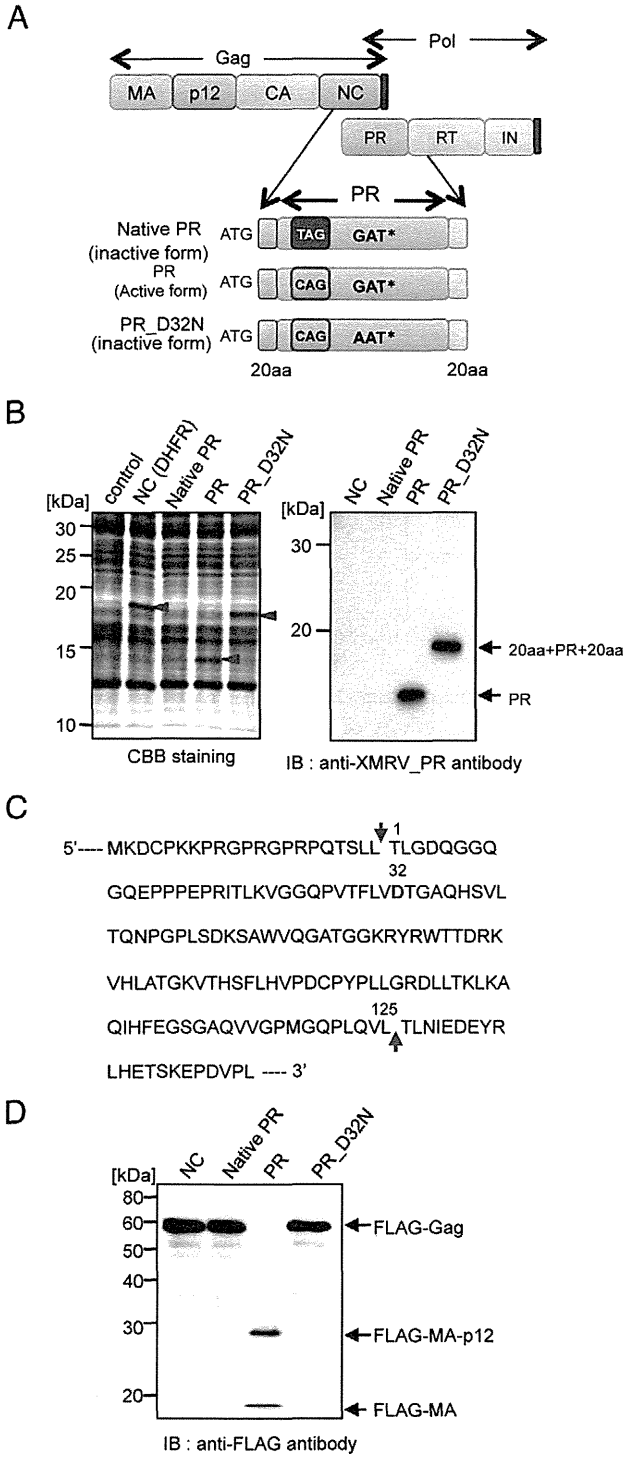


**Fig. 1 – Synthesis of enzymatically active XMRV protease (PR) by wheat cell-free protein production system. A. Construction of expression vector of XMRV PR for wheat cell-free synthesis. TAG (stop) codon between Gag and PR was substituted for CAG (Q) codon. Non-active form of PR was generated by the substitution of AAT (N) for catalytic center GAT (D). B. XMRV PRs (DHFR as a negative control) were separated by SDS-PAGE followed by CBB-stained (left panel) and immunoblotting using anti-XMRV PR antibody (right). The arrows depict protein products. C. Amino acid sequence of XMRV PR. The arrows indicate self-cleavage site in XMRV PR. D. Cleavage of XMRV Gag by XMRV PR produced by wheat cell-free system. XMRV PR was incubated with cell-free synthesized FLAG-tagged XMRV Gag (arrow), and the cleaved Gag was detected by immunoblot analysis with anti-FLAG antibody.**

## 4. Discussion

In the current study, we developed a cell free protease assay with XMRV PR which can evaluate the cleavage activity via AlphaScreen or immunoblot analysis. We demonstrate the advantage of utilizing wheat cell-free system that was able to systematically produce catalytically active viral protease with a large amount for biochemical assays. Furthermore, our in vitro enzymatic assay revealed that APV is a potent inhibitor of XMRV PR. We have also delineated the physical interaction between APV and XMRV PR and identified the amino acid residues involved in the binding. Finally, we demonstrated the substrate specificity for XMRV PR as compared with HIV-1 PR. These results might reveal that our current assay system is a powerful tool to characterize viral proteases and to screen their specific inhibitors.

XMRV is a virus that was generated as the result of a unique recombination event between two endogenous MLV-like viruses in a nude mouse carrying the CWR22 prostate cancer xenograft [6]. Although XMRV is an unusual virus, XMRV has been associated with prostate cancer [2]. In fact, the human cell line 22Rv1, which was established from a human prostate tumor (CWR22), produces infectious XMRV particles [30]. While the absence of XMRV in non-prostatic tumors

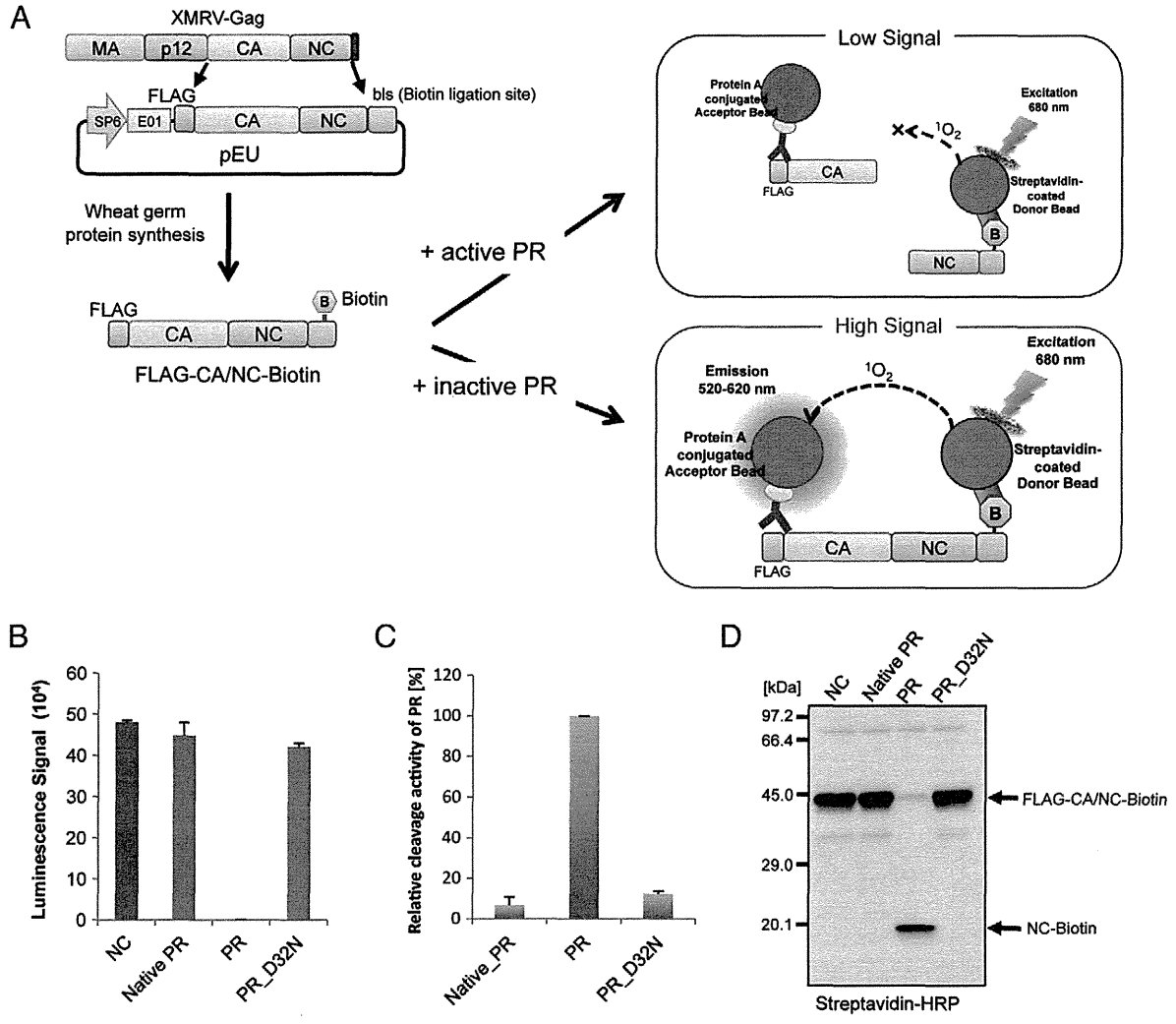


**Fig. 2 – Development of a cleavage activity assay for XMRV PR using the luminescent assay AlphaScreen. A. Schematic diagram of the substrate construction of XMRV PR and detection system for the cleavage activity of XMRV PR by luminescent analysis. Substrate was designed as XMRV Gag capside (CA) and nucleocapside (NC) flanked by N-terminal FLAG and C-terminal biotin (FLAG_CA-NC_biotin). PR was incubated with the substrate, for 1 h at 37 °C. Subsequently, protein A-conjugated acceptor beads with anti-FLAG antibody and streptavidin coated donor beads were added and bound to the tagged substrate. Upon laser excitation, Donor beads convert ambient oxygen to a singlet oxygen. In the case of non-activity PR, singlet oxygen transfers across to activate Acceptor beads and subsequently emit light at 520–620 nm. In the case of active PR, no light is produced because the singlet oxygen can not transfer from Donor beads to Acceptor beads due to the distance (>200 nm). B,C,D. Cleavage activity of XMRV PR was quantitated by the luminescent assay (Fig.2B). Actual cleavage of XMRV Gag substrate was also confirmed by immunoblotting with streptavidin-HRP (Fig.2D). The arrow indicates the band for the non-cleaved substrates (FLAG_CA/NC_biotin).**

remains controversial [31], XMRV can however proliferate in other human prostate cancer cells such as LNCaP or PC3 without severe cytopathic effects [32]. Such conditions of persistent infection without cell death could conceivably lead to prolonged exposure of host cell proteins to XMRV PR, increasing their susceptibility to cleavage with oncogenic consequences. The important question remains, however, as to whether this virus has indeed tumorigenic capability. Previous reports have indicated that XMRV integration is characterized by a strong preference for transcriptional start sites, CpG islands, and DNase-hypersensitive regions, all features that are frequently associated with structurally-open transcription regulatory regions of the chromosome in prostate cancer cells [33]. Integration of XMRV occurs preferentially in actively-transcribed genes and gene-dense regions within the chromosome [33]. Oncogenic properties of XMRV have been investigated in cell culture models. Although XMRV has been reported to lack direct transforming activity, the virus is able to induce low rates of transformation in cultured fibroblast cells [34]. Therefore, the molecular link between XMRV infection and cell transformation merits further investigation.

Our current data demonstrates that APV is a potent antagonist of XMRV PR. During the preparation of this manuscript, Li et al. reported the crystal structure of complexes

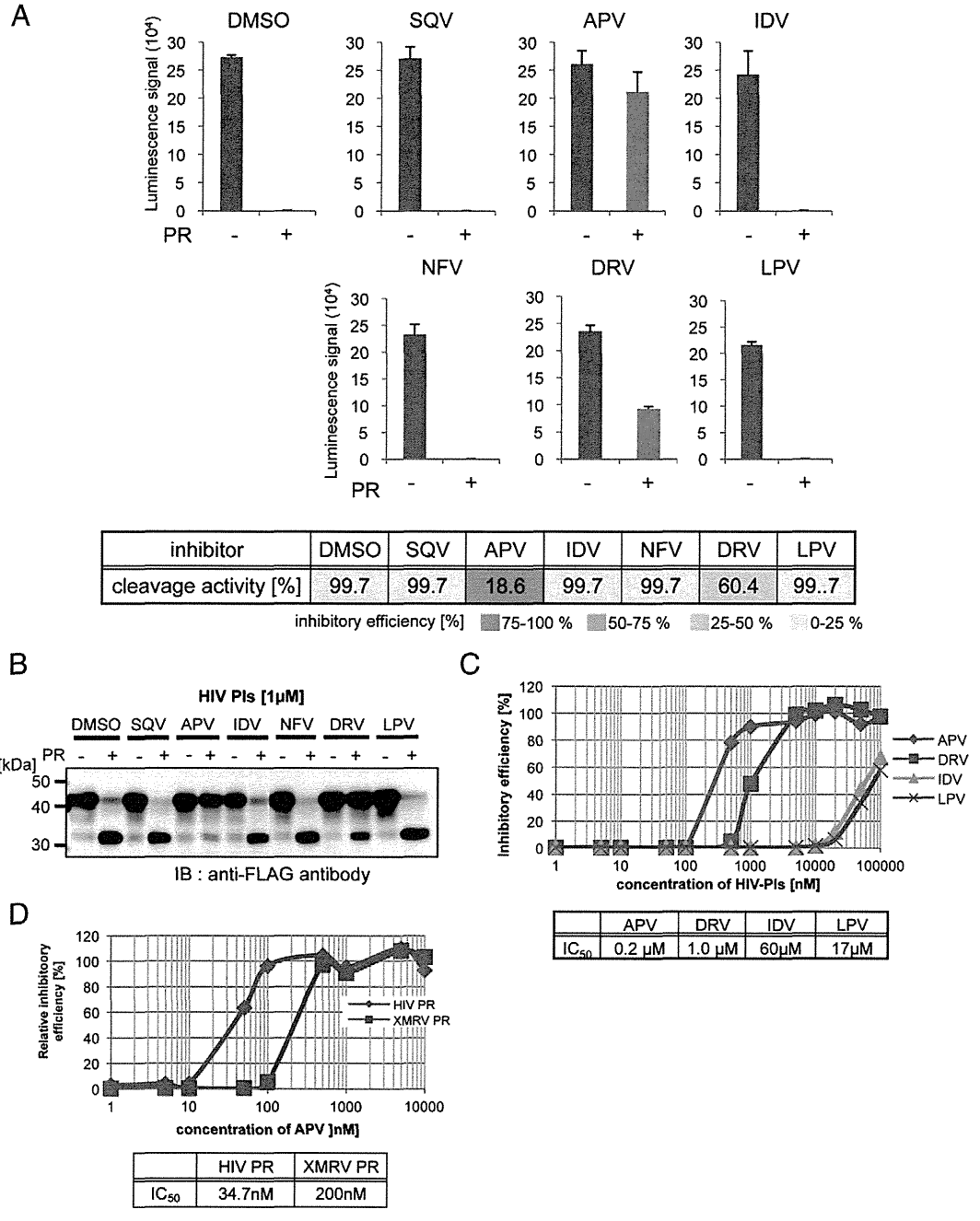


**Fig. 3 – Drug screening for XMRV PR based on the cleavage activity. A,B. XMRV protease (+) or DHFR (–) was pre-incubated with indicated HIV PIs (SQV, saquinavir; APV, amprenavir; IDV, indinavir; NFV, nelfinavir ; DRV, darunavir; LPV, lopinavir; 1 μM each) and then subjected to AlphaScreen. Luminiscent AlphaScreen signal (upper panel) and relative enzymatic activity (lower panel) were listed. C. Conformation of the cleavage of the tester polypeptide by immunoblot analysis with anti-FLAG antibody. D. Dose–response curve of XMRV PR with HIV PIs using AlphaScreen (upper panel). $IC_{50}$ values were calculated for each inhibitor (lower panel). E. Dose–response curve of XMRV PR and HIV-1 PR with APV using AlphaScreen (upper panel). $IC_{50}$ values were calculated for each protease (lower panel).**

formed between XRMV PR and several protease inhibitors, including APV [24,35]. In the current study we moved a step closer to clarifying the molecular interactions between XMRV PR and APV during drug-resistance, by developing an effective cell-free in vitro protease assay for XMRV PR. This assay revealed that an Ala57Val substitution induced significant drug-resistance to APV regardless of the integrity of the protease activity. The data indicates that this cell-free assay is useful for analyzing the drug-resistance properties of retroviral proteases.

Proteases often modify the activities of their target substrates [36]. Identification of the specific substrates cleaved by viral PR is of great significance for understanding the molecular etiology of virus infection. Proteomic studies with mass spectrometry could, theoretically, exhaustively identify the cellular proteins cleaved

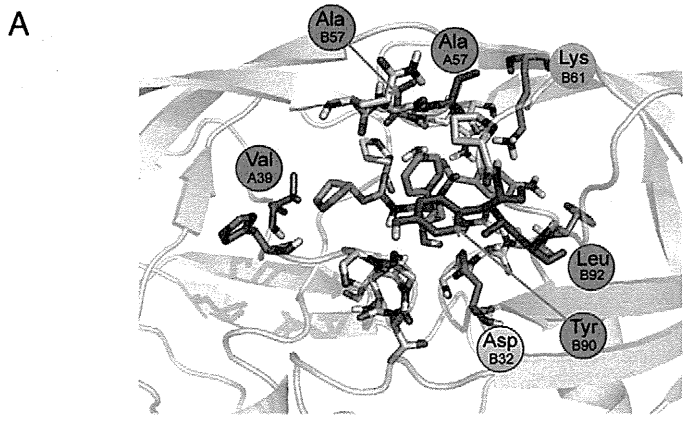


B

```
                10          20          30          40          50
XMRV  TLGDQGGQGQ EPPPEPRITL KVGGQPVTFL VDTGAQHSVL TQNPGPLSDK
HIV-1 -----PQITL W--QRPLVTI KIGGQLKEAL LDTGADDTVL EEMSLPGRWK
                5          13          23          33          43
               60          70          80          90         100
XMRV  SAWVQGATGG KRYRWTTDRK VHLATGKVTH SFLHVPDCPY PLLGRDLLTK
HIV-1 PKMIGGIGGF IKVRQYDQIL IEICGHKAIG TVL-VGPTPV NIIGRNLLTQ
               53          63          73          82          92
              110         120    125
XMRV  LKAQIHFEGS GAQVVGPMGQ PLQVL
HIV-1 IGCTLNF--- ---------- -----
           99
```

C

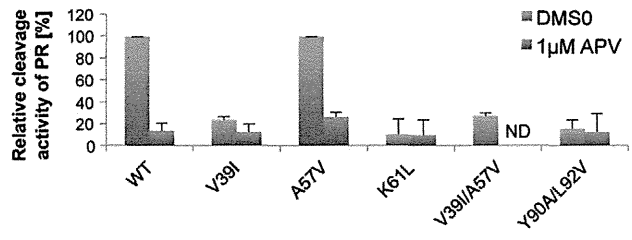


| | WT | V39I | A57V | K61L | V39I/A57V | Y90A/L92V |
|---|---|---|---|---|---|---|
| cleavage activity [%] | 99.7 | 23.5 | 99.7 | 10.3 | 27.0 | 15.6 |
| inhibitory efficiency [%] | 13.9 | 53.0 | 26.6 | 95.0 | 0.0 | 81.7 |

cleavage activity [%] 75-100 % 50-75 % 25-50 % 0-25 %

inhibitory efficiency [%] 75-100 % 50-75 % 25-50 % 0-25 %

D

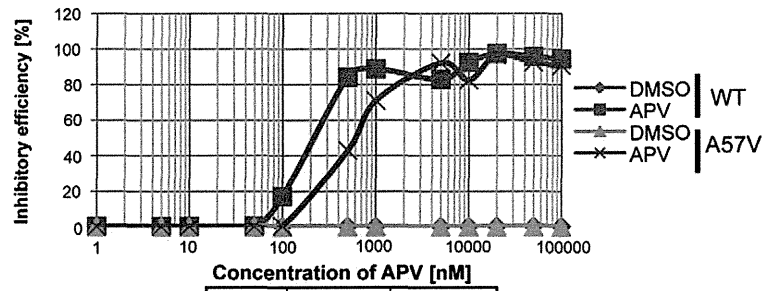


| | WT | A57V |
|---|---|---|
| $IC_{50}$ | 200 nM | 596 nM |

**Fig. 4 – Prediction of the amino acid residues of XMRV PR interacting with APV. A. The predicted 3D-structure for the interaction between XMRV PR and APV. This homology modeling was based on the HIV-1 PR and APV complex as a template. B. Sequence alignment of XMRV PR and HIV-1 PR. The amino acids related to interaction of APV with HIV-1 PR and the corresponding amino acids in XMRV PR are highlighted with red letters. C. Cleavage activity of XMRV PR-WT and its mutants in the presence of 1 μM APV or equivalent amount of DMSO (control). Lower panel is cleavage activity and inhibitory efficiency (APV value/DMSO value) for each XMRV PR. D. Dose–response curve of the inhibitory rate of PR-WT or PR-A57V by APV.**

A

| No. | Symbol | Gene bank accession No. | aa | Da | Cleavage by XMRV PR |
|---|---|---|---|---|---|
| 1 | ANXA1 | BC001275 | 346 | 38714 | No |
| 2 | GJB2 | BC017048 | 226 | 26215 | No |
| 3 | ARL11 | BC013150 | 196 | 21391 | Yes |
| 4 | RND3 | BC012513 | 244 | 27368 | No |
| 5 | FHIT | BC032336 | 147 | 16858 | No |
| 6 | KCNRG | BC032343 | 272 | 31048 | No |
| 7 | SFRP1 | BC036503 | 314 | 35386 | No |
| 8 | WNT5A | BC064694 | 380 | 42339 | No |
| 9 | SMAD3 | BC050743 | 425 | 48081 | No |
| 10 | p21 | BC000312 | 164 | 18119 | No |
| 11 | NME1 | BC000293 | 152 | 17149 | No |
| 12 | MAL | BC000458 | 153 | 16714 | No |
| 13 | SPINT2 | BC001668 | 252 | 28228 | No |
| 14 | SLC39A1 | BC003152 | 324 | 34250 | No |
| 15 | CHEK2 | BC004207 | 543 | 60915 | No |
| 16 | DKK3 | BC007660 | 350 | 38291 | Yes |
| 17 | TIMP3 | BC014277 | 211 | 24145 | No |
| 18 | BAX | BC014175 | 192 | 21184 | Yes |
| 19 | ALPL | BC021289 | 524 | 57305 | No |
| 20 | CST6 | BC031334 | 149 | 16510 | No |
| 21 | KLF5 | BC042131 | 457 | 50792 | No |
| 22 | CAV1 | BC082246 | 178 | 20472 | No |
| 23 | PTEN | BC005821 | 403 | 47166 | Yes |
| 24 | TP53 | BC003596 | 393 | 43653 | No |

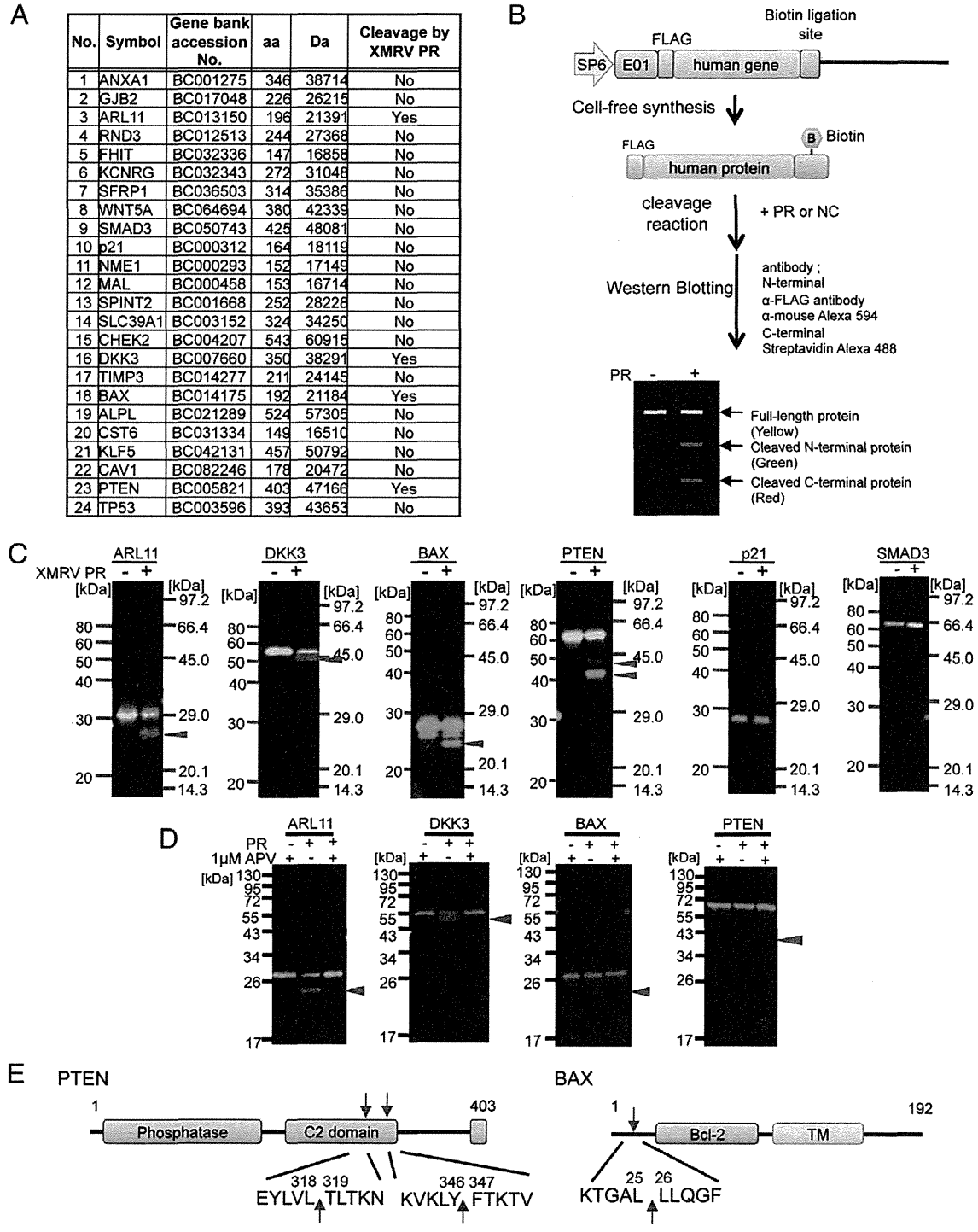


**Fig. 5 – Screening of host proteins cleaved by XMRV PR in vitro. A. The list of human tumor suppressor proteins tested in this study. B. Scheme of the tester proteins construction and the cleavage assay system by immunoblotting. The genes were amplified by PCR with primer sets containing either FLAG or biotin ligation site (bls) in the flanking sequence, respectively. The recombinant host proteins flanking FLAG and biotin (FLAG-X-biotin) were incubated with XRMV PR at 37 °C for 2 h followed by SDS-PAGE. The proteins were detected using anti-FLAG-Alexa592 antibody (green) and Alexa488-conjugated streptavidin (red). Full-length protein is seen as a yellow band. C. Tester proteins were treated with XMRV PR or carrier. 2-color immunoblot analysis was performed as in Materials and methods. D. Tester proteins were treated with XMRV PR in the absence or presence of amprenavir. Immunoblot analysis was performed as in C. E. Identification of the cleavage site in the XMRV PR amino acid sequence.**

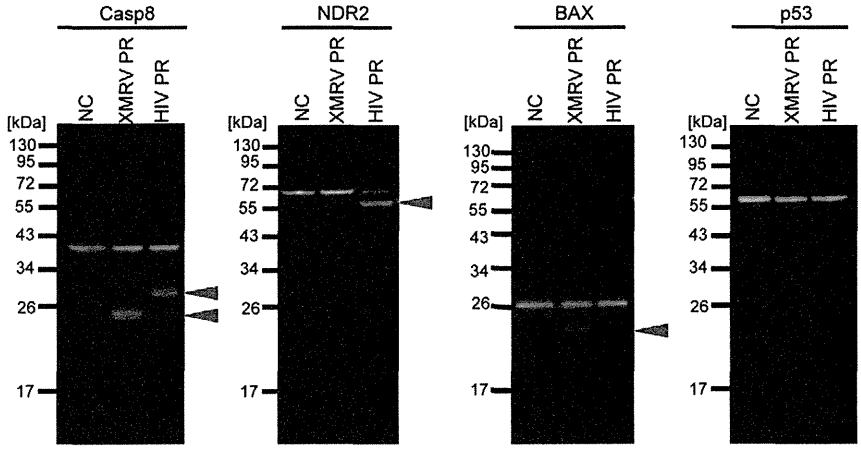


**Fig. 6 – Comparative analysis of host proteins cleaved by XMRV PR and HIV-1 PR. The recombinant host proteins flanking FLAG and biotin (FLAG-X-biotin) were incubated with either XRMV PR or HIV-1 PR at 37 °C for 2 h followed by SDS-PAGE. The proteins were detected using anti-FLAG-Alexa592 antibody (green) and Alexa488-conjugated streptavidin (red). Full-length protein is seen as a yellow band. Arrows depict the cleavage products.**

by retroviral proteases in infected cells. However, this cell-based will run into difficulty identifying individual substrates if several host proteases act simultaneously on the substrate. To circumvent this potential problem we developed the cell-free in vitro method for the identification of substrates cleavable by XMRV PR. Wheat extracts purified rarely include endogenous proteases that can interfere with the proteolytic reaction, making them suitable for the cell-free protease assay.

Tumor suppressor proteins play a major role in preventing tumor initiation. Our current results demonstrate that XMRV PR can cleave PTEN and BAX tumor suppressors as well as the intrinsic substrate XMRV Gag. It has been reported that the C-terminal region of PTEN is important for the protein's stability, and the C-terminal deletion mutant is degraded rapidly in cells [37]. Since XMRV cleaves within the C-terminal region, the native function and stability of PTEN might be abrogated by XMRV infection. The N-terminal region of BAX has been demonstrated to mediate its activity in apoptosis [38]. We demonstrated in the present study that XMRV PR can cleave the N-terminal region of BAX, suggesting that XMRV infection might affect the activity of BAX protein.

A biochemical approach to the evaluation of PR-inhibitor susceptibility has been attempted previously using several related methods [39,40]. The essence of each of these procedures is the synthesis of catalytically-active PR and substrate peptide and inhibitor in vitro, and measurement of the amount of substrate cleavage. The advantage of this approach is that it can directly detect the catalytic activity of PR. However, it is often difficult to produce sufficient quantities of enzymatically active viral PR in conventional cell-based protein expression systems such as *E. coli* or insect cells. In our current study, we successfully created catalytically-active XMRV PR in a cell-free system that, when mixed with a reporter substrate flanked with N- and C-terminal fluorophores, substrate cleavage could be assayed by AlphaScreen or 2-color IB. This approach directly evaluates the cleavage activity of the PR and, in addition, cleavage sites can be estimated by the size of cleavage products. The current availability of full-length cDNA libraries, derived from higher eukaryotes, will facilitate the in vitro synthesis of full-length proteins, making this cell-free system approach could further be applicable to the assay of a broad range of, not only viral, but also host proteases.

## 5. Conclusion

We have delineated the molecular and enzymatic characteristics of XMRV PR by utilizing wheat-germ cell-free protein synthesis and AlphaScreen. Furthermore, we have developed an in vitro cleavage assay for drug screening based on the enzymatic activity. Our results suggest that XMRV-protease cleavage of certain host proteins and inhibited by APV. Further in vivo studies with XMRV-infected cells will be necessary to confirm a molecular link between XMRV and human diseases.

## Acknowledgments

We thank Drs. G. Quinn, Y. Kojima and A. Kudo for the discussion and comments. This work was supported in part by grants from the Ministry of Education, Culture, Sports, Science and Technology of Japan and Research Grants on HIV/AIDS Health Labour Sciences Research Grant from The Ministry of Health Labour and Welfare of Japan to A.R. MK was supported by grants from MEXT, JST, Sumitomo-Denko and Iwatani.

## REFERENCES

[1] Urisman A, Molinaro RJ, Fischer N, Plummer SJ, Casey G, Klein EA, et al. Identification of a novel Gammaretrovirus in prostate tumors of patients homozygous for R462Q RNASEL variant. PLoS Pathog 2006;2:e25.
[2] Schlaberg R, Choe DJ, Brown KR, Thaker HM, Singh IR. XMRV is present in malignant prostatic epithelium and is

associated with prostate cancer, especially high-grade tumors. Proc Natl Acad Sci U S A 2009;106:16351–6.
[3] Knox K, Carrigan D, Simmons G, Teque F, Zhou Y, Hackett Jr J, et al. No evidence of murine-like gammaretroviruses in CFS patients previously identified as XMRV-infected. Science 2011;333:94–7.
[4] van Kuppeveld FJ, van der Meer JW. XMRV and CFS–the sad end of a story. Lancet 2012;379:e27–8.
[5] Simmons G, Glynn SA, Komaroff AL, Mikovits JA, Tobler LH, Hackett Jr J, et al. Failure to confirm XMRV/MLVs in the blood of patients with chronic fatigue syndrome: a multi-laboratory study. Science 2011;334:814–7.
[6] Paprotka T, Delviks-Frankenberry KA, Cingoz O, Martinez A, Kung HJ, Tepper CG, et al. Recombinant origin of the retrovirus XMRV. Science 2011;333:97–101.
[7] Groom HC, Yap MW, Galao RP, Neil SJ, Bishop KN. Susceptibility of xenotropic murine leukemia virus-related virus (XMRV) to retroviral restriction factors. Proc Natl Acad Sci U S A 2010;107:5166–71.
[8] Dong B, Silverman RH. Androgen stimulates transcription and replication of xenotropic murine leukemia virus-related virus. J Virol 2010;84:1648–51.
[9] Abudu A, Takaori-Kondo A, Izumi T, Shirakawa K, Kobayashi M, Sasada A, et al. Murine retrovirus escapes from murine APOBEC3 via two distinct novel mechanisms. Curr Biol 2006;16:1565–70.
[10] Ventoso I, Blanco R, Perales C, Carrasco L. HIV-1 protease cleaves eukaryotic initiation factor 4G and inhibits cap-dependent translation. Proc Natl Acad Sci U S A 2001;98:12966–71.
[11] Zaragoza C, Saura M, Padalko EY, Lopez-Rivera E, Lizarbe TR, Lamas S, et al. Viral protease cleavage of inhibitor of kappaBalpha triggers host cell apoptosis. Proc Natl Acad Sci U S A 2006;103:19051–6.
[12] Takai K, Sawasaki T, Endo Y. Practical cell-free protein synthesis system using purified wheat embryos. Nat Protoc 2010;5:227–38.
[13] Kamura N, Sawasaki T, Kasahara Y, Takai K, Endo Y. Selection of 5′-untranslated sequences that enhance initiation of translation in a cell-free protein synthesis system from wheat embryos. Bioorg Med Chem Lett 2005;15:5402–6.
[14] Tadokoro D, Takahama S, Shimizu K, Hayashi S, Endo Y, Sawasaki T. Characterization of a caspase-3-substrate kinome using an N- and C-terminally tagged protein kinase library produced by a cell-free system. Cell Death Dis 2010;1:e89.
[15] Akagi T, Shimizu K, Takahama S, Iwasaki T, Sakamaki K, Endo Y, et al. Caspase-8 cleavage of the interleukin-21 (IL-21) receptor is a negative feedback regulator of IL-21 signaling. FEBS Lett 2011;585:1835–40.
[16] Sakuma R, Sakuma T, Ohmine S, Silverman RH, Ikeda Y. Xenotropic murine leukemia virus-related virus is susceptible to AZT. Virology 2010;397:1–6.
[17] Sawasaki T, Kamura N, Matsunaga S, Saeki M, Tsuchimochi M, Morishita R, et al. Arabidopsis HY5 protein functions as a DNA-binding tag for purification and functional immobilization of proteins on agarose/DNA microplate. FEBS Lett 2008;582:221–8.
[18] Takahashi H, Nozawa A, Seki M, Shinozaki K, Endo Y, Sawasaki T. A simple and high-sensitivity method for analysis of ubiquitination and polyubiquitination based on wheat cell-free protein synthesis. BMC Plant Biol 2009;9:39.
[19] Sawasaki T, Gouda MD, Kawasaki T, Tsuboi T, Tozawa Y, Takai K, et al. The wheat germ cell-free expression system: methods for high-throughput materialization of genetic information. Methods Mol Biol 2005;310:131–44.
[20] Sawasaki T, Hasegawa Y, Tsuchimochi M, Kamura N, Ogasawara T, Kuroita T, et al. A bilayer cell-free protein synthesis system for high-throughput screening of gene products. FEBS Lett 2002;514:102–5.
[21] Matsuoka K, Komori H, Nose M, Endo Y, Sawasaki T. Simple screening method for autoantigen proteins using the N-terminal biotinylated protein library produced by wheat cell-free synthesis. J Proteome Res 2010;9:4264–73.
[22] Baker D, Sali A. Protein structure prediction and structural genomics. Science 2001;294:93–6.
[23] Labute P. The generalized Born/volume integral implicit solvent model: estimation of the free energy of hydration using London dispersion instead of atomic surface area. J Comput Chem 2008;29:1693–8.
[24] Li M, Dimaio F, Zhou D, Gustchina A, Lubkowski J, Dauter Z, et al. Crystal structure of XMRV protease differs from the structures of other retropepsins. Nat Struct Mol Biol 2011;18:227–9.
[25] Johnson VA, Brun-Vezinet F, Clotet B, Gunthard HF, Kuritzkes DR, Pillay D, et al. Update of the drug resistance mutations in HIV-1. Top HIV Med 2008;16:138–45.
[26] Alvarez E, Castello A, Menendez-Arias L, Carrasco L. HIV protease cleaves poly(A)-binding protein. Biochem J 2006;396:219–26.
[27] Bellecave P, Sarasin-Filipowicz M, Donze O, Kennel A, Gouttenoire J, Meylan E, et al. Cleavage of mitochondrial antiviral signaling protein in the liver of patients with chronic hepatitis C correlates with a reduced activation of the endogenous interferon system. Hepatology 2010;51:1127–36.
[28] Nie Z, Phenix BN, Lum JJ, Alam A, Lynch DH, Beckett B, et al. HIV-1 protease processes procaspase 8 to cause mitochondrial release of cytochrome c, caspase cleavage and nuclear fragmentation. Cell Death Differ 2002;9:1172–84.
[29] Devroe E, Silver PA, Engelman A. HIV-1 incorporates and proteolytically processes human NDR1 and NDR2 serine-threonine kinases. Virology 2005;331:181–9.
[30] Knouf EC, Metzger MJ, Mitchell PS, Arroyo JD, Chevillet JR, Tewari M, et al. Multiple integrated copies and high-level production of the human retrovirus XMRV (xenotropic murine leukemia virus-related virus) from 22Rv1 prostate carcinoma cells. J Virol 2009;83:7353–6.
[31] Stieler K, Schindler S, Schlomm T, Hohn O, Bannert N, Simon R, et al. No detection of XMRV in blood samples and tissue sections from prostate cancer patients in Northern Europe. PLoS One 2011;6:e25592.
[32] Rodriguez JJ, Goff SP. Xenotropic murine leukemia virus-related virus establishes an efficient spreading infection and exhibits enhanced transcriptional activity in prostate carcinoma cells. J Virol 2010;84:2556–62.
[33] Kim S, Kim N, Dong B, Boren D, Lee SA. Das Gupta J, et al. Integration site preference of xenotropic murine leukemia virus-related virus, a new human retrovirus associated with prostate cancer. J Virol 2008;82:9964–77.
[34] Metzger MJ, Holguin CJ, Mendoza R, Miller AD. The prostate cancer-associated human retrovirus XMRV lacks direct transforming activity but can induce low rates of transformation in cultured cells. J Virol 2010;84:1874–80.
[35] Li M, Gustchina A, Matuz K, Tozser J, Namwong S, Goldfarb NE, et al. Structural and biochemical characterization of the inhibitor complexes of xenotropic murine leukemia virus-related virus protease. FEBS J 2011;278:4413–24.
[36] Etlinger JD, Gu M, Li X, Weitman D, Rieder RF. Protease/inhibitor mechanisms involved in ATP-dependent proteolysis. Rev Biol Cell 1989;20:197–216.
[37] Georgescu MM, Kirsch KH, Akagi T, Shishido T, Hanafusa H. The tumor-suppressor activity of PTEN is regulated by its carboxyl-terminal region. Proc Natl Acad Sci U S A 1999;96: 10182–7.
[38] Toyota H, Yanase N, Yoshimoto T, Moriyama M, Sudo T, Mizuguchi J. Calpain-induced Bax-cleavage product is a more potent inducer of apoptotic cell death than wild-type Bax. Cancer Lett 2003;189:221–30.
[39] Dreyer GB, Metcalf BW, Tomaszek Jr TA, Carr TJ, Chandler 3rd AC, Hyland L, et al. Inhibition of human immunodeficiency virus 1 protease in vitro: rational design of substrate analogue inhibitors. Proc Natl Acad Sci U S A 1989;86:9752–6.
[40] Hoffmann D, Buchberger B, Nemetz C. In vitro synthesis of enzymatically active HIV-1 protease for rapid phenotypic resistance profiling. J Clin Virol 2005;32:294–9.

Available online at www.sciencedirect.com

SciVerse ScienceDirect

Current Opinion in Chemical Biology

# Ribosomal production and *in vitro* selection of natural product-like peptidomimetics: The FIT and RaPID systems

Christopher J Hipolito and Hiroaki Suga

Bioactive natural product peptides have diverse architectures such as non-standard sidechains and a macrocyclic backbone bearing modifications. *In vitro* translation of peptides bearing these features would provide the research community with a diverse collection of natural product peptide-like molecules with a potential for drug development. The ordinary *in vitro* translation system, however, is not amenable to the incorporation of non-proteinogenic amino acids or genetic encoding of macrocyclic backbones. To circumvent this problem, flexible tRNA-acylation ribozymes (flexizymes) were combined with a custom-made reconstituted translation system to produce the flexible *in vitro* translation (FIT) system. The FIT system was integrated with mRNA display to devise an *in vitro* selection technique, referred to as the random non-standard peptide integrated discovery (RaPID) system. It has recently yielded an *N*-methylated macrocyclic peptide having high affinity ($K_d$ = 0.60 nM) for its target protein, E6AP.

**Address**
Department of Chemistry, Graduate School of Science, The University of Tokyo, Tokyo 113-0033, Japan

Corresponding author: Suga, Hiroaki (hsuga@chem.s.u-tokyo.ac.jp)

**Current Opinion in Chemical Biology** 2012, **16**:196–203

This review comes from a themed issue on
Biocatalysis and Biotransformation
Edited by Jon S Thorson and Ben Shen

Available online 6th March 2012

1367-5931/$ – see front matter


**DOI 10.1016/j.cbpa.2012.02.014**

## Introduction

Bioactive natural product peptides are biosynthesized by either ribosomal translation machinery or nonribosomal peptide synthetases (NRPSs) and derivatized by post-translational modification enzymes or tailoring NRPS enzymes, respectively [1]. Unlike ordinary peptides, these 'non-standard' peptides are chemically diversified with D-amino acids, unique sidechains, *N*-methylation, and macrocyclic backbones (Figure 1). In the case of NRPSs, this diversity is largely attributed to the multidomain NRPSs' ability to activate and modify amino acids before condensation. Domains are grouped into modules, and each module is in general responsible for the activation, modification and condensation of a single amino acid. Nature arranges these modules into an assembly line so that an exact peptide sequence can be produced in an NRPS-templated manner. The idea of producing custom non-standard peptides or their *de novo* libraries has attracted many researchers and driven efforts toward engineering NRPSs, but manipulating the modular NRPS components to create tailored non-standard peptides has thus far met limited success owing to their mechanistic and functional complexities. Presumably, directed evolution of NRPSs, similar to the recent work reported by Fischbach *et al.* [2] as well as Evans *et al.* [3], may lead to a solution of this herculean challenge in order to achieve the goal of constructing *de novo* libraries in the future.

Biosynthetic pathways involving post-translational modification enzymes are less complex than those involving NRPSs. In fact, genetic and mechanistic studies on such enzymes have increased our knowledge of essential recognition elements in substrates, enabling us to design non-natural substrates. Moreover, recent studies using synthetic peptides as well as coupling with *in vivo* incorporation of an artificial amino acid has allowed for the expansion of substrate repertoires [4–7]. Thus, continuing such efforts will lead us to the goal of synthesis of *de novo* libraries and, ultimately, discovering bioactive compounds with new chemical scaffolds against therapeutic targets of interest.

As a completely different technology, recent advances in artificial manipulation of the genetic code have shown the potential to produce natural product-like non-standard peptides by using translation machinery (*vide infra*). In this technology, unlike the above two biosynthetic processes, the sequences of such non-standard peptides are encoded in messenger RNA (mRNA) or its parental DNA. This feature facilitates the construction of their *de novo* libraries with high sequence complexities and, moreover, enables us to devise a one-pot screening (or selection) system to discover active non-standard peptides. In this review, we shall focus on discussing this emerging new technology.

## Genetic code reprogramming as a distinct alternative approach

Genetic code reprogramming, which allows for a variety of non-standard amino acids to be incorporated by using sense codon suppressions, is a technique that was introduced within the last decade [8,9]. Genetic code reprogramming in general requires the use of a reconstituted *in vitro* translation system [10]. For instance, Forster *et al.* demonstrated in 2003 that reconstitution of only limited members of *Escherichia coli* translation factors (initiation

**Figure 1**

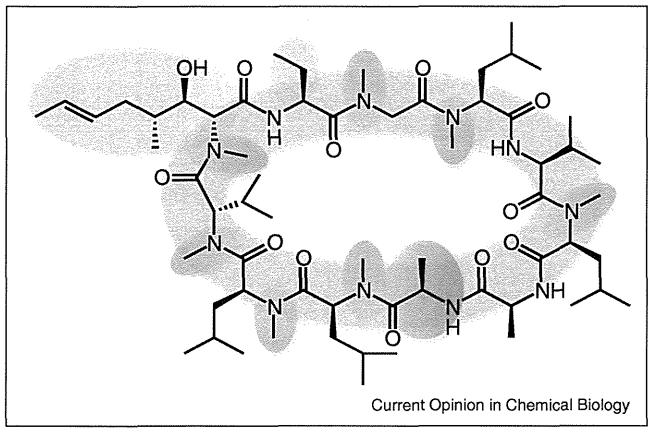


Structure of cyclosporin A, a nonribosomal peptide. Non-standard sidechains, *N*-methyl groups, a D-amino acid, and a macrocyclic peptide backbone are highlighted by yellow ovals, orange ovals, a blue oval, and a green doughnut, respectively.

factors IF1–3, elongation factors EF-Tu, G, and Ts) together with fMet-tRNA$^{fMet}_{CAU}$ and 70S ribosomes constituted a translation system with universally vacant elongator codon boxes. Subsequent refilling of three vacant boxes with three artificial amino acids by the addition of their aminoacyl-tRNAs resulted in successful expression of fMet-initiated tri-peptides or tetrapeptides [8]. Although this experiment was performed under single turnover conditions, it represented the first example of formatting codon boxes and reprogramming the genetic code by reconstituting the translation apparatus.

Since the Forster's demonstration, two methods, which are technically more advanced but both achieved through genetic code reprogramming, have been reported. Szostak *et al.* used a reconstituted *E. coli* translation system based on the protein synthesis using recombinant elements (PURE) system in which certain amino acids were depleted to make vacant codon boxes [10–12]. This method relied on the ability of some aminoacyl-tRNA synthetases (ARSs) to mischarge a wide array of non-standard amino acids onto cognate tRNAs under conditions lacking the cognate proteinogenic amino acids. The resulting mischarged non-standard amino acids were assigned to the vacant codon boxes by the tRNAs, thus allowing for expression of peptides containing multiple non-standard amino acids. The virtue of this method is the simplicity; the undesired amino acids were simply substituted with non-standard amino acids in the PURE system, and peptide translation could be performed. On the contrary, shortcomings also exist in this method. Since the choices of non-standard amino acids rely on the mischarging properties of ARSs, they often fall into the category of 'proteinogenic-like' non-standard amino acids. Moreover, even though a certain set of proteinogenic amino acids was not added to the PURE system, because ribosomes and ARSs are not completely proteinogenic amino acid-free (*i.e.* they carry over some amino acids into the PURE system), contaminating amino acids could compete with non-standard amino acids for incorporation. Particularly, since the proteinogenic amino acids are intrinsically much better substrates for ARSs, elongation factors, and ribosomes, their trace amount of competitive incorporation against non-standard amino acids is difficult to avoid. Therefore, the application of this method to *de novo* library synthesis of non-standard peptides must be carefully tuned in a balance of choice between non-standard amino acids and codons having the least contaminants of cognate proteinogenic amino acids.

The second method, developed by our group, also uses a reconstituted *E. coli* translation system, but the genetic code reprogramming relies on the preparation of desired non-standard aminoacyl-tRNAs by a *de novo* catalytic system based on flexizymes [13]. Flexizymes are flexible tRNA acylation ribozymes of which the prototype ribozyme was artificially selected from a random pool of RNA sequences. Reviews on the history and catalytic abilities of flexizyme can be found in recently written articles [14–17]. In brief, flexizymes are short ribonucleotides consisting of 45 or 46 nucleotides in length, and recognize specific leaving groups of amino acid esters. Since flexizymes strictly recognize neither sidechain nor amino group of given amino acids, they are able to charge a wide variety of non-proteinogenic (as well as proteinogenic) amino acids onto tRNAs. Moreover, the recognition of tRNA by flexizyme is dictated by the interaction of flexizyme's 3′-end motif with tRNA's 3′-end sequence via only 3 base pairs, that is, neither body nor anticodon sequences of tRNAs are involved. This feature grants flexizymes the ability to charge any kind of tRNA. Integration of the flexizymes with a reconstituted translation system, such as the PURE system, allowed us to devise a highly versatile peptide expression system with regards to the choice of amino acids and tRNAs. We refer to this system as the flexible *in vitro* translation (FIT) system [18].

## The flexible *in vitro* translation (FIT) system

The FIT system is a translation apparatus comprised of two main groups of components. One group is made up of reconstituted *E. coli* translation components (IF1–3, EF-Tu, EF-G, EF-Ts, release factors RF2 and RF3, ribosome recycling factor RRF, methionine trans-formylase MTF and select ARSs), 70S ribosome, and desired proteinogenic amino acids [18]. By omitting the components (amino acids and ARSs) corresponding to specific codon boxes, vacant codon boxes are made available for non-proteinogenic amino acids. The other group of components is made up of the desired non-proteinogenic amino acids charged, by a flexizyme or flexizymes, onto orthogonal tRNAs (otRNAs) that correspond to the vacant codon boxes and are inert with the ARSs present in the FIT system. Their addition to the above custom-made translation apparatus complements